UNIVERSITÀ DEGLI STUDI DEL PIEMONTE ORIENTALE
"AMEDEO AVOGADRO"
FACOLTÀ DI SCIENZE M.F.N.

DIPARTIMENTO DI SCIENZE E INNOVAZIONE TECNOLOGICA

CORSO DI DOTTORATO DI RICERCA IN:
SCIENZE AMBIENTALI (Acque interne e agroecosistemi)

CICLO XXVI

ISOLATION, STRUCTURAL AND BIOCHEMICAL CHARACTERIZATION OF PLANT PSII-LHCII SUPERCOMPLEXES

Candidato : Simone BARERA
Responsabile scientifico: Prof. Roberto BARBATO
Responsabile scientifico esterno: Dott.ssa Cristina PAGLIANO
Coordinatore del corso: Prof. Giorgio MALACARNE
Settore scientifico disciplinare: BIO 04

TABLE OF CONTENTS

LIST OF ABBREVIATIONS

APS	Ammonium persulphate
ATP	Adenosine triphosphate
BCIP	5-bromo-4- chloro-indolyl phosphate
Chl	Chlorophyll
Cyt	Cytocrome
DCBQ	2,6-dichloro benzoquinone
DCMU	3-(3,4-dichlorophenyl)-1,1-dimethylurea
DM	dodecyl-D-maltoside
DTT	Dithiothreitol
EM	Electron microscope
ESI	Electron Spray Ionization
EDTA	Ethylenediaminetetraacid
FeCN	Ferrycianide ($K_3Fe(CN)_6$)
FNR	Ferredoxin-$NADP^+$-Reductase
GTP	Guanosine triphosphate
HEPES	N-2-hydrossiethilpiperazine N'-2-etansulphonic
LHCI-II	Light Harvesting Complex I-II
LMM	Low Molecular Masses
MALDI-TOF	Matrix-assisted laser desorption ionization/time of flight
MES	2-[N-morpholino]ethanesulfonic
NADP	Nicotinamide adenine dinucleotide
NBT	Nitro blue tetrazolium
OEC	Oxygen-evolving complex
P680	Primary electron donor in PS II
PC	Plastocyanine
PQ	Plastoquinone
Pheo	Pheophytin, localized in D1 protein
PSI	Photosystem I
PSII	Photosystem II
Q_A	The first quinone electron acceptor in PS
Q_B	The second quinine electron acceptor in
SDS-PAGE	Sodium dodecyl sulfate polyacrylamide
Temed	N,N,N- tetramethylethylendiamine
TMBZ	Tetramethyl benzidine
Tricine	N-[2-hydroxy-1,1- bis(hydroxymethyl)
Tris	Tris-[hydroxymethyl]amino-methane

ABSTRACT

In the first part of this thesis work, they have been investigated the solubilizing properties of α-DM and β-DM on the isolation of photosynthetic complexes from pea thylakoids membranes maintaining their native architecture of stacked grana and stroma lamellae. Exposure of these stacked thylakoids to a single step treatment with increasing concentrations (5–100 mM) of α-DM or β-DM resulted in a quick partial or complete solubilization of the membranes. Regardless of the isomeric form used: 1) at the lowest DM concentrations only a partial solubilization of thylakoids was achieved, giving rise to the release of mainly small protein complexes mixed with membrane fragments enriched in PSI from stroma lamellae; 2) at concentrations above 30 mM a complete solubilization occurred with the further release of high molecular weight protein complexes identified as dimeric PSII, PSI-LHCI and PSII–LHCII supercomplexes. It has been identified in 50 mM of both detrgents the minimal concentration that fully solubilized PSII-LHCII supercomplexes. In the second part of this work they have been characterized, in terms of polypeptide composition, purity and functionality by using biochemical techniques, two forms of PSII-LHCII supercomplexes isolated via sucrose gradient centrifugation from solubilized *Pisum sativum* thylakoid with 50 mM α- and β-n-dodecil maltoside. In according to the previous results, to isolate the supercomplexes they have been solubilized directly thylakoids instead of PSII membranes (BBYs), in order to minimize the possibility of detergent-induced artefacts and they have been used stacked membranes in order to avoid destabilization of the interaction of LHCII with the PSII core. The isolated supercomplexes haven't shown any ATP-ase and PSI contaminations. Both supercomplexes have shown an identical set of LMM subunits. The supercomplex isolated with α-DM was larger and more intact, in terms of OEC and Lhcb subunits, than the supercomplex isolated with β-DM. The supercomplex isolated with α-DM has shown an higher activity than of those isolated with β-DM. In the last part of the work they have been structurally characterized both isolated supercomplexes by using EM single particle analysis. The EM data have shown that the supercomplexes isolated with α-DM was a $C_2S_2M_2$ while those isolated with β-DM was a C_2S_2 supercomplex. They have been obtained the 2D projection maps and the 3D reconstructions maps and angular reconstitution at 30 Å (for the $C_2S_2M_2$) and at 28 Å (for the C_2S_2).

LIST OF ORIGINAL PUBLICATIONS

This thesis is based on the following publications (in attachment):

Pagliano, C., Barera, S., Chimirri, F., Saracco, G., Barber, J. (2012). Comparison of the α and β isomeric forms of the detergent n-dodecyl-D-maltoside for solubilizing photosynthetic complexes from pea thylakoid membranes. Biochim. Biophys. Acta 1817: 1506-1515.

Barera, S., Pagliano, C., Pape, T., Saracco, G., Barber, J. (2012). Characterization of PSII-LHCII supercomplexes isolated from pea thylakoid membrane by one-step treatment with α- and β-dodecyl-D-maltoside. *Phil. Trans. R. Soc. B* 367:3389-3399.

Pagliano, C., Nield, J., Marsano, F., Pape, T., Barera, S., Saracco G.,Barber J. (2013). Proteomic characterization and three-dimensional electron microscopy study of PSII-LHCII supercomplexes from higher plants. *Biochim. Biophys. Acta* Nov 16. doi:pii: S0005-2728(13)00189-8. (*in press*).

GENERAL INTRODUCTION

1. GENERAL INTRODUCTION:

1.1 Photosynthesis (Light reactions):

Photosynthesis is the process by which light energy is converted into chemical energy. The overall chemical reaction of oxygenic photosynthesis is the sunlight-driven, chlorophyll-sensitised transformation of water and atmospheric carbon dioxide to make energy-storing carbohydrates, and oxygen as a by-product. Photosynthetical reactions take place inside the thylakoid membranes and they are catalized by four multi-subunit membrane protein complexes (PSII, cytochrome b_6f, PSI and ATP-ase).

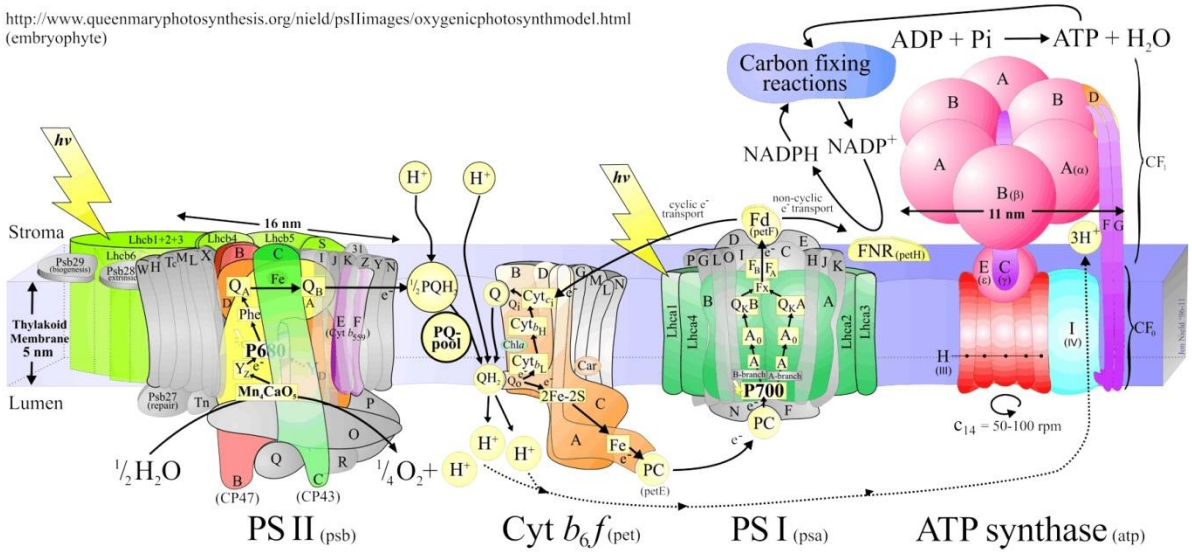

Figure 1.1 Cartoon model of the functional organization of photosynthetic thylakoid membranes in oxygenic organisms (Copyright © Jon Nield, Queen Mary, University of London, UK).

The most important reaction of photosynthesis is the water oxidation carried out by Oxygen Evolving Complex (OEC), the oxidizing side of PSII.

1.1.1 Thylakoids organization:

Thylakoid membranes are organized in two main regions: staked region (grana) and unstacked region (stroma lamellae). In higher plants grana are a well organized piles of stacked thylakoid membranes in wich are located PSII complexes (dimer and supercomplexes). Grana stacks are linked by stroma lamellae in wich are located mainly PSI and ATP-ase. The 3D architecture of the granum–stroma

assembly and the entire thylakoid membrane network is complicate and interesting, especially because of the ability of the membranes to undergo reversible changes in folding and organization under varying environmental conditions. Recently many efforts are aimed at determining of the 3D organization of the thylakoid membranes, in particular the capacity to form grana stacks. One of the main consequences of stacking is the physical separation of PSI and PSII. The chloroplast ultrastructure changes from shade to sun plants, in fact as an adaptation to low light conditions, some plants have evolved extensive granal stacking in order to maximize the thylakoidal area involved in capturing solar energy (Anderson et al. 1975). The sun plants instead, living under excess light, have less appressed thylakoid membranes (Boardman, 1977), which could be an adaptation to maximize the space for the enzymes that are required for carbon fixation reactions. The organization of the thylakoid membranes rapidly and reversibly responds to changes in light intensity and quality not only in palnts growth in different light conditions, but the changes are visible in the alternation from day to night. The dynamics in the lateral distribution of the photosynthetic protein complexes in the thylakoid membrane most probably have a vital role in regulation of the functions, maintenance, and efficiency of the photosynthetic apparatus. Recent studies (Danielsson et al, 2006) have demonstrated that PSII distribution is well defined and it is correlated to the chloroplast ultrastructure. In the grana core are located mainly PSII-LCHII supercomplexes, while from these region towards the lamellae region are located PSII dimer and PSII monomer. The regulation of the chloroplast ultrastructure and the disposition of the water-splitting cofactors of the PSII complex inside the thylakoid membranes are mechanisms finely regulated and are essential to limitate photodamage. When the excess of light damage PSII, the damaged protein migrates from grana to stroma membranes, where the non-functional complexes are disassembled, damaged subunits are replaced with newly synthesized ones, and after reassembly the PSII complex finally migrates back to grana membranes. (Mulo et al. 2008). They have been proposed two models of the chloroplast ustrastructure the elical model and the fork model rapresented in figure 1.2 A and B.

The helical model was derived from EM studies of thin sections and serial sections of chemically fixed thylakoid membranes. As it is visible in figure 1.2, the stroma thylakoids are enfolded around the granal stacks in the form of multiple right-handed helices. The helical arrangement of the stroma thylakoids around grana was further supported by electron microscopy techniques including scanning electron microscopy and freeze-fracture EM (Staehelin et al. 1996). More recently tomography data revealed that there are fewer connections between one particular granum thylakoid and its surrounding

stroma thylakoids. Also the number of connected grana thylakoids in a stack by one spiral stromal thylakoid seems to be lower than previously thought.

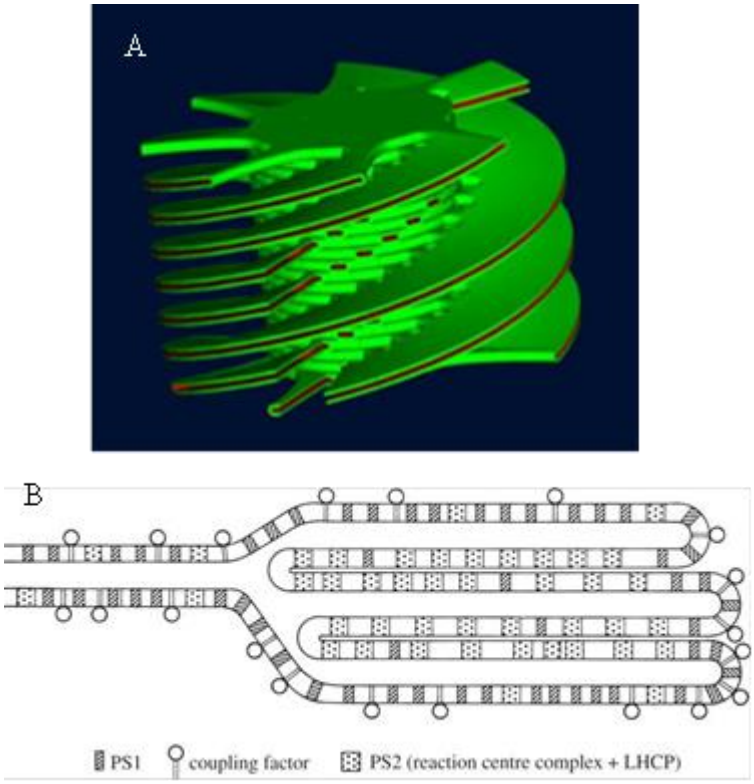

Figure 1.2 A. Two current models for the 3D organization of thylakoid membranes in plant chloroplasts. (A) The helical model (Mustàrday et al. 2003) (B) The fork model (Andersson and Anderson, 1980).

Electron tomography studies have demonstrated that the dimensions of the connections between the stroma and grana thylakoids are more variable in size (Daum et al. 2010, Austin and Staehelin, 2011).
The fork or folded membrane model was proposed at the beginning of 80's to illustrate the lateral heterogeneity in the distribution of PSII and PSI in the thylakoid membrane (Andersson and Anderson, 1980). In this model, represented in figure 1.2 B, the stroma membranes bifurcate and make a fork, which connects two adjacent grana thylakoids within a stack. The fork model was proposed not based on direct structural data but the fork motif was observed in many micrographs, including those of thin serial sections (Mustàrdy et al. 2008). Strong evidences for the existence of the fork at the granum–stroma assembly were provided by cryo tomography on cryo immobilized and freeze-substituted sections of intact leaves (Shimoni et al. 2005).

1.1.2 Linear electron transfer

Each of the four complex embedded in the thylakoidal membranes plays a distinct role in the electron transfer chain (ETC). PSII cointains a special pair chl called P680 that generates strong oxidant able to extract electrons from water and split it in O_2 and protons (H^+) using Calcium-Manganese cluster (donor side). The electrons come from water are collected by plastoquinone pool. The plastoquinoles are then reoxidized by the Cyt b_6f complex and the electrons are collected by plastocyanin. During electron transport, Cyt b_6f releases H_+ in the lumen generating a H_+ electrochemical gradient across the thylakoidal membrane. This ΔH_+ proton motive force (pmf) is dissipated by the ATP-ase to form ATP. The plastocyanin, reduced by Cyt b_6f, donates the electrons to the photo-oxidized P700 of the PSI which, on photon absorption, reduces ferredoxin. In conclusion ferredoxin is oxidized by FNR to obtain NADPH. Linear electron transfer is described by the Z scheme, in wich it is possible, observing the redox potential, the relationships between the involved electron acceptors and donors (figure 1.3).

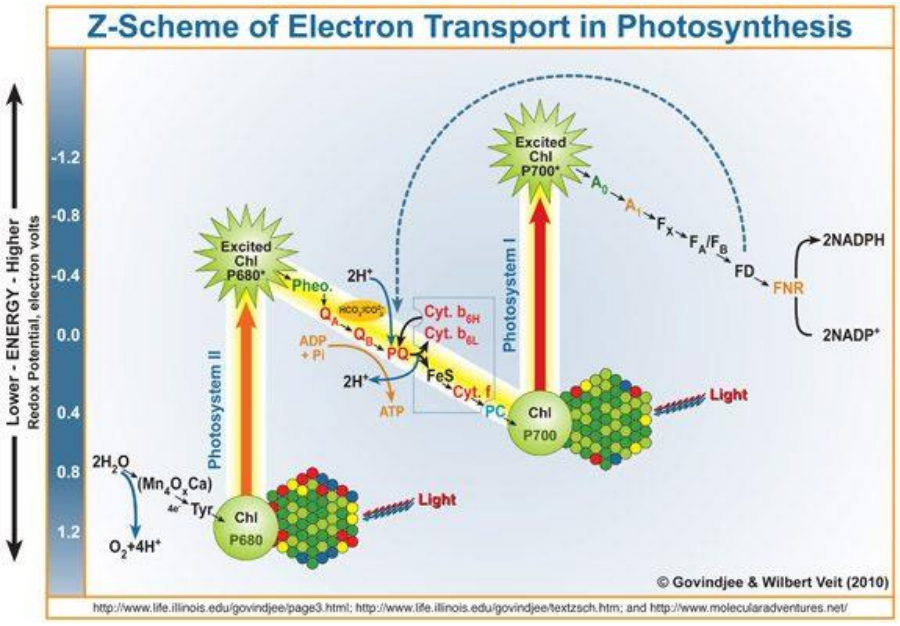

Figure 1.3 Representation of the Z-scheme (Copyright © Govindje & Wilbert Veit 2010).

1.1.3 Cyclic electron transfer

During the light phase of the photosynthetical process not all the harvested light is adsorbed, a fraction is dissipated as fluorescence, the process by which chlorophylls release, with a longer wavelength, the energy derived from light absorption. Another fraction is dissipated as heat. The remaining portion is used for photochemical reactions. The percentage of not adsorbed light changes as a consequence of

light intensity and environmental conditions such as temperature, salt stress or drought. The excess of light absorption during the photosynthesis light reaction could lead to damage the photosynthetic apparatus via ROS generation, accordingly, it must be tuned and balanced. There are three mechanisms in the oxygenic photosynthetic organisms by which the excess of light is dissipated an the synthesis of ATP and NADPH is regulated: cyclic electon transfer (CET), state transition and water-water cycle.

Cyclic electron transport have been discovered fifty years ago, until now they have been characterized two redundant routes for electrons cycling around PSI: the first one involves an NAD(P)H dehydrogenase (NDH) encoded by chloroplast and the other one is dependent on the PGR proteins (DalCorso et al. 2008). The electrons derived from the PSI reducing side are transferred back to the plastoquinones pool in both cases. In this way the proton gradient across the thylakoid membrane is enhanced generating more ATP.

With the first route mediating by NDH, called Chlororespiration, plants controls ATP/NADPH ratio in order to low the stromal over-reduction due to excessive light absorption with respect to the need of reducing equivalents (Shikanai, 2007).

The second one (PGR mediated route), instead, is less characterized, but seems to be connected to the thermal dissipation mechanisms of excessive absorbed light called nonphotochemical quenching (NPQ). A major component of NPQ, measured as a quenching of fluorescence emission, is energy-dependent thermal dissipation quencing (qE), which is related to the xanthophyll cycle. Thermal dissipation mechanisms involves, during the xanthophyll cycle, Violaxanthin deepoxidase (npq1) and protonation of PsbS, a subunit of PSII which is also known as npq4, and, as a consequence, this latter reaction is pH dependent (Li et al. 2000). In mediated PGR pathway PGR5, a membrane protein, is involved in the transfer of electrons from ferredoxin to plastoquinone. This alternative electron transfer pathway, whose molecular identity has long been unclear, is known to function in vivo in cyclic electron flow around photosystem I. It has been proposed (Shikanai, 2007) that the PGR5 pathway contributes to the generation of a ΔpH that induces thermal dissipation when Calvin cycle activity is reduced. Under these conditions, the PGR5 pathway also functions to limit the overreduction of the acceptor side of PSI, thus preventing photosystem I photoinhibition. This pathway is Antimicyn A-sensitive, indicating a direct connection with the Q cycle of Cyt b_6f in higher plants (Takahashi, 2009). The pgr5 mutant of *Arabidopsis thaliana* has been described as being deficient in cyclic electron flow around PSI, however, the precise role of the PGR5 protein remains unknown. Recently it has been examined PGR pathway by measurements of the kinetics of P700 oxidation in far red light and re-reduction following oxidation in the presence of DCMU in intact leaves of pgr5 and wild type A.

thaliana. The measurements has demonstrated that the mutant is able to perform cyclic electron flow at a rate similar to the wild type. The PGR5 protein is therefore not essential for cyclic flow. However, cyclic flow is affected by the pgr5 mutation under conditions where this process is normally enhanced in wild type leaves, high light or low CO_2 concentrations resulted in enhancement of cyclic electron flow. This suggests a different capacity to regulate cyclic flow in response to environmental stimulation in the mutant. The pgr5 mutant is inefficient in maintaining the right plastidial redox potential, in fact, the electron transport chain is reduced in most cases. In addition to the membrane protein PGR5, there is another transmembrane protein called PGRL1 present in thylakoids of *Arabidopsis thaliana*. It has been demonstrated that plants lacking PGRL1 shown a similar beahvior to PGR5-deficient plants. Recent studies confirm that PGRL1 and PGR5 interact physically and associate with PSI.

1.2 PSII structure and functions:

1.2.1 General overview:

PSII is a membrane protein complex embedded in the thylakoid membrane, it is a water-plastoquinone oxido-reductase. The reaction catalized by this enzyme is the one of most important for the life on our planet. The release of dioxygen, during light phase of photosynthesis, created an oxygenic atmosphere allowing a widely diversified life, based on mitochondrial-oxidative phosphorylation. The great importance of PSII for the life on earth justifies the considerable efforts that have been made to obtain further details, using biochemical, biophysical and genetic approaches, about its structure and the oxygene evolution reaction.

Recently, the attention of many researchers has been driven towards the possibility of mimic the water splitting activity. In order to reach this goal it is necessary a deep knowledge of the structure of the PSII catalytic site. In the past the first direct structural information about PSII was derived from electron microscopy (EM) via freeze fracture studies on thylakoid membranes (Staehelin et al. 2003), followed by the imaging isolated PSII particles (Hankamer et al. 1997). PSII dimeric structure, and its water-splitting activity, are conserved among all the photosynthetic oxygenic organisms. Thus the sequences of the intrinsic PSII subunits are highly conserved in all oxygen evolving autotrophs, are encoded by plastidial genes in green algae and higher plants, whereas the extrinsic proteins are nuclear-encoded and show high variability among oxygenic photosynthetic organisms (Ishihara et al. 2007). The little variability between plant PSII and cyanobacteria PSII has allowed to complement the electron

crystallographic studies of the higher plant PSII core dimer with X-ray crystallographic data obtained from cyanobacterium PSII crystals.

Several X-ray crystallographic structures are available for cyanobacterial PSII (Zouni et al. 2001; Jordan et al. 2001; Ferreira et al. 2004; Kamiya and Shen, 2003; Guskov et al. 2009;) and also the detailed structure of LHCII has been resolved (Liu et al. 2004; Standfuss et al. 2005; Yan et al. 2007). Actually, the crystal structure of PSII isolated from T. vulcanus has been refined to 1.9 Å giving more information about the positioning of the water molecules and giv further detail about the OEC (Umena et al. 2011).

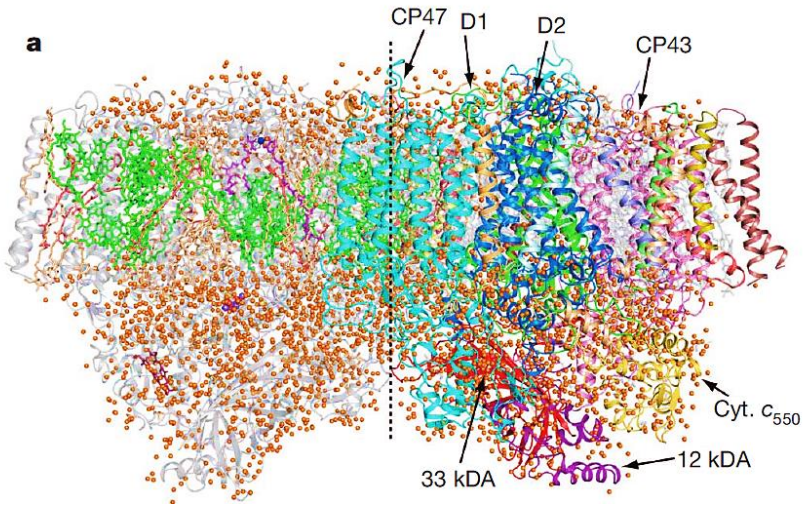

Figure 1.4. Crystal structure of PSII isolated from T. vulcanus at 1.9 Å (Umena et al. 2011).

Unfortunaltely the complete structure of higher plant PSII hasn't been resolved. Therefore the combination of structural information about the cyanobacterial PSII core and higher plant LHCII with experimental biochemical data has made it possible to model the structure of the PSII-LHCII complex of higher plants (Nield and Barber, 2006). In general, solving of the structure of PSII at the highest resolution possible has become one of the most important goals of modern biology. Knowing the exact structure of the water-splitting apparatus of PSII would pave the way to development of photolytic bio-mimicking devices to produce hydrogen or electricity from water and sunlight.

Even if the high resolution 3D structure of cyanobacteria PSII dimer revealed all the positions of the atoms inside the oxygen evolving complex and the water molecules, the water splitting reaction carried out by manganese cluster, is still an unclear process and it needs further studies.

1.2.2 PSII polypeptide composition and arrangement

It has been widely believed that the PSII complex normally functions as a dimer and the monomeric complex may be an intermediate form in the normal assembly pathway or in the damage-repair cycle (Barbato et al. 1992; Hankamer et al. 1997).

PSII complex is composed by more than 20 subunits and many cofactors. PSII subunits can be divided in 3 groups: core complex proteins, low molecular mass subuinits, oxygen evolving extrinsic subunits.

Core complex proteins:

PSII reaction center (RC) is composed by two homologues five- α helix trans membrane proteins with molecular mass around 39 kDa D1 and D2 (encoded from psbA and psbD genes rispectively), it contains all the cofactors involved in the electron transfer chain, from water to plastoquinones. Proteins D1 and D2 are higly conserved in fact they are remarkably similar to the L and M subunits of the purple bacteria *Rhodopseudomonas sphaeroides* reaction center (Barber et al. 1987). They contain a pheophytin molecule, a β carotene molecule (Loll et al. 2005), three chlorophyll a molecules. Inside the loops between the IV and V helices on the stromal side of these proteins there are binding sites for a plastoquinone molecule. Protein D1 binds the majority of the cofactors involved in PSII electron transport chain: Y Z is Tyr161, P680 is Chl a molecule ligated by His198 (called PD1), Pheo D1 is molecule of pheophytin bounded by Tyr126 and Glu130 and a Q B site where plastoquinone molecules are bounded. D1 contains an other Chl molecule called Chl D1 and bind the manganese cluster in the C-terminal region. All of residues implicated in this bind, located close to the surface of the CD lumenal α-helix of the D1 subunit, are nearly absolutely conserved with very little variation observed in dinoflagellates (Takishita and Uchida, 1999). Moreover D1 protein binds two chloride atoms near to the manganese cluster (Murray et al. 2008; Umena et al. 2011) and a non-haem Fe, normally redox inactive, which is positioned equal distance between Q A and Q B.

Another important property of D1 is the rapidly assembly-disassembly in the thylakoid membrane. This is due to the fact that PSII is susceptible to photoinibition and to protect entire system, D1 is degradated in order to regulate the electron transport chain. The degradation, synthesis and reinsertion of this protein into the PSII in plants is finely regulated. During the turnover Met1 is cleaved and its N-terminal Thr can be acetylated and reversibly phosphorylated. (Michel et al. 1988; Pursiheimo et al. 1998; Vener et al. 2001; Turkina et al. 2006).

The D2 proteins conatins two Chl a molecules, P D2 and Chl D2 , which together with P D1 and Chl D1 form the cluster constituting P680 and the QA site. The D2 protein also contributes ligands for the non-haem Fe, and is involved in binding chloride through side chain.

Similarly to D1, in higher plants and green algae (but not in cyanobacteria) the D2 undergoes reversible acetylation and phosphorylation of its N-terminal Thr residue (Michel et al. 1988; Pursiheimo et al. 1998; Vener et al. 2001; Turkina et al. 2006).

CP47 and CP43, products of the psbB and psbC genes, are the core complex antenna proteins, they transfer excitons derived by light absorption to P680 at two opposite sides of the RC. They are structurally homologous, having a molecular weight of ~ 56 and 50 kDa respectively, six α–helices each of them and sixteen and fourteen chlorophyll a molecules respectively.

CP47 protein has 16 Chl a molecules and 5 β-carotenes. It has a very large lumenal loop joining transmembrane between helices V and VI, consisting of 200 amino acids arranged in two long and four short helices as well three β-sheets. The large loop indirectly takes part in the water oxidation reaction by interacting with the D2 protein, which is adjacent to it.

CP43 (PsbC), after post-translational processing, contains 470 amino acids it is homologous to CP47 in that it has six transmembrane a-helices arranged in the same way but located on the D1-side of the RC. It also contains 13 Chl a molecules and binds 5 b-carotene molecules. It has a large lumenal loop like CP47 but slightly smaller. CP43 protein contains two long and three short helices one of which contains the highly conserved motif which provides a ligand to the manganese cluster. Altough there are some differencese with CP47, the main function remains the same: CP43 acts as a light-harvesting system for PSII and its presence is also necessary for water-splitting activity.

Low molecular mass subuinits:

Inside the PSII core complex, apart from D1, D2, CP43 and CP47 there are many subunits called Low Molecular Mass (LMM) because of their molecular weight its from about 3 kDa to 12 kDa. Up to now the knowledge about their function is very low; it seems, however, that most of these LMM polypeptides are not involved in the electron transfer but, instead, are structural components.

The first evidence for low molecular mass subunits associated with the PSII complex was presented by Ljungberg and his co-workers who isolated a hydrophilic 5-kDa protein (corresponding to PsbTn) from PSII and shown that the PSII complex contained several other small, unidentified subunits. This small polypeptides were named, according to their apparent molecular masses, the 10, 8, 7, 6.5, 5.5-, 5 and 4-

kDa proteins. Recently they have been added 6.8, 3.7 and the 3.2 kDa proteins to the list of small subunits in PSII.

Several of the low molecular mass subunits of PSII were sequenced and the first corresponding gene products, PsbK and PsbI were identified. The protein nomenclature was correlated to the gene names to avoid the confusing names related to the apparent molecular masses of the proteins. Dramatic improvements and developments have been made in protein detection and identification techniques during the last decade. Highly sensitive fluorescence techniques combined with the latest improvements in ion mass spectrometric techniques, which allow the detection and identification of some femtomoles of proteins (roughly corresponding to 0.1 ng), now complement the traditional Coomassie brilliant blue staining. These new techniques have confirmed that PSII contains a large set of low molecular mass subunits. Molecular biological methods have also yielded new insights into this group of PSII subunits. The LMM proteins identified are encoded by the psbE, psbF, psbH, psbR, psbI, psbJ, psbK, psbL, psbM, psbN, psbT, psbX, psbW and psbZ genes.

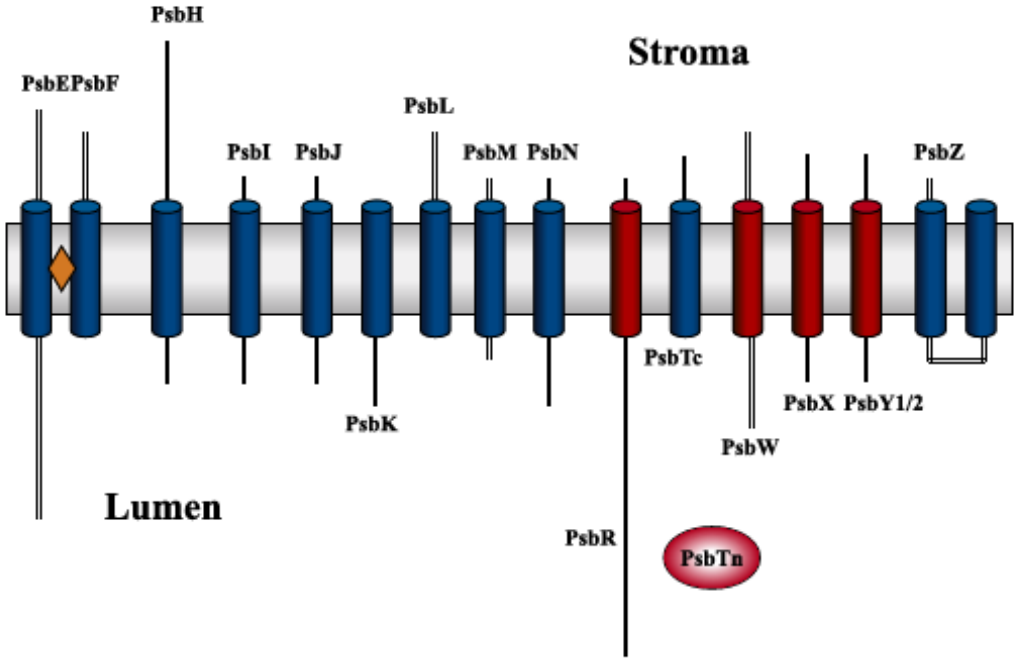

Figure 1.5 Cartoon representation of the transmembrane elices of the LMM proteins (Shi and Schroeder, 2004).

PsbE and PsbF

The genes psbE and psbF encode for α and β subuinits of Cytochrome b 559 (Cyt b 559) with molecular masses of 9 and 4 kDa, respectively and each of these polypeptides has one transmembrane helix. The Cyt b 559 is closely associated with PSII in all oxygenic photosynthetic organisms. The α and β subunits of the Cyt b 559 are components of the minimal PSII reaction center complex that is still capable of primary charge separation (Nanba et al. 1987). Cyt b 559 is a b-type cytochrome, but it has a unique feature with respect to its midpoint reduction potential (Em). High-, low- and intermediate-potential forms of Cyt b 559 have been observed in intact chloroplasts, PSII membranes and isolated D1/D2/ Cyt b 559 complexes. The function of Cyt b 559 has been unknow for a long time, but structural details suggest that Cyt b 559 could participate in a secondary electron transfer pathway within PSII (Heber et al. 1979). These observations and the results of other studies on Cyt b 559 mutants indicate that Cyt b 559 is involved in protecting PSII from photoinhibition (Poulson et al. 1995). In addition, evidence from site-directed mutagenesis in Synechocystis 6803 suggests that Cyt b 559 is required for the assembly of functional PSII complexes. (Morais et al. 1998).

PsbH

The PsbH protein was identified in higher plant chloroplasts and initially called 10- or 9-kDa phosphoprotein. It is encoded by the plastome in algae and higher plants and it is present also in cyanobacteria. The protein contains 63-90 amino acids, depending on the species, with molecular masses between 7.0 and 9.9 kDa. PsbH is an intrinsic membrane protein with a single transmembrane helix and its N-terminal region has been suggested to be exposed to the stromal side of the thylakoid membrane. In higher plants, the protein is located close to Cyt b 559 and PsbX (Buchel et al. 2001), its phosphorylation sites of PsbH are located at the N-terminus and this reversible phosphorylation is light-dependent and redox-controlled (Michel et al. 1987). Recent studies on PSII complexes isolated from spinach suggest that PsbH, together with other PSII phosphoproteins, may be required for D1 protein turnover by regulating dimeric and monomeric PSII transition through their phosphorylation and dephosphorylation. This has been further substantiated by the recent demonstration that PsbH is required for the rapid degradation of the photodamaged D1 protein and insertion of newly synthesized D1 into the thylakoid membrane. In summary, the PsbH protein is essential for PSII activity in eukaryotes. It may play a role in regulating PSII assembly/stability and may also be involved in repair of photodamaged PSII under high light.(Kruse et al. 1997, Bergantino et al. 2003).

PsbI

The PsbI protein, called also 4.8-kDa protein, is encoded by the plastome. PsbI is highly conserved in higher plants and cyanobacteria. The protein contains at least 38 amino acids with molecular masses ranging between 4.1 and 4.5 kDa. Sequence analysis indicates that it has a single transmembrane span. The N-terminus of this protein is formyl-Met and is located on the stromal side of the thylakoid membrane and analysis of its cross-linked proteins indicates that the nearest neighbors of PsbI are D2 and the a subunit of Cyt b 559 (Tomo et al. 1993). The function of PsbI has been investigated in Cyanobacteria. Inactivation of the psbI gene in Synechocystis 6803 and T. elongatus strain BP-1 caused similar reductions in PSII activity. In the case of T. elongatus DpsbI mutant, no dimeric PSII could be isolated. It was suggested that while PsbI is not essential for PSII photochemistry in cyanobacteria, it may be involved in processes that help to optimize PSII function, such as the dimerization of PSII or stabilization of PSII dimers (Ikeuchi et al. 1995).

PsbJ

PsbJ is one of the most hydrophobic proteins in the thylakoid membrane, containing 39-42 amino acid residues, with a molecular mass between 4.0 and 4.4 kDa. Sequence analysis suggests that the protein has a single transmembrane helix with its N-terminus extending to the stromal side. The PsbJ function is controversial even if there are many evidence that the inactivation of the psbJ gene reveal phenotype with low PSII oxygen evolution caused by the reduced amount of functional PSII complexes. (Lind et al. 1993, Regel et al. 2001).

PsbK

The chloroplast PsbK protein has been found in PSII core complexes from the thermophilic cyanobacteria and higher plants. The PsbK precursor contains a hydrophobic presequence ranging from 5 to 24 amino acids long, and some of the longer presequences have a putative transmembrane span that may play a role in the insertion of the protein in the thylakoid membrane. In all species examined so far mature PsbK protein contains 37 amino acids and has molecular masses between 4.1 and 4.3 kDa. Accordingly, it is the most conserved small protein in PSII. The Arabidopsis PsbK shares 76% identity with the Synechocystis 6803 homolog. PsbK has been recently found to be tightly associated with CP43 (Sugimoto and Takahashi, 2003). Deletion of the psbK gene in Chlamydomonas destabilized the PSII complex, and the amount of PSII in the resulting mutants was less than 10% of

wild-type levels.The transformate bacteria were unable to grow photoautotrophically and no PSII activity was detected, suggesting that this protein is indispensable for PSII function in Chlamydomonas (Takahashi et al. 1994). Biochemical analysis of subcore complexes of PSII from spinach has shown that dimeric CP47-reaction center complexes contain the small proteins PsbK and PsbL, together with 1-2 molecules of plastoquinone.The monomeric complexes instead do not contain PsbK.According to these results, it has been suggested that the PsbK protein is involved in binding plastoquinone and in maintaining the dimeric organization of PSII (Zheleva et al. 1998).

PsbL

PsbL protein is encoded by the plastome, it contains 37-39 amino acid residues with molecular masses between 4.3 and 4.5 kDa depending on the species. Primary sequence analysis suggests that PsbL has one transmembrane helix and it has also been suggested that the N-terminus of the protein is located at the stromal side of the thylakoid membrane. PsbL is present in both PSII core complexes of higher plants and cyanobacteria only in the dimeric form, indicating that the PsbL protein may have a role in maintaining PSII dimeric organization (Zheleva et al. 1998). The Synechocystis 6803 PsbL mutant shown the total loss of PSII-mediated oxygen evolution, and it appear to be unable to grow photoautotrophically. Interestingly, no binding of herbicides that normally bind D1/D2 proteins was detected in these mutants, despite immunological detection of D1 and D2 protein. This was suggested to be due to changes on the acceptor side of PSII (Anbudurai and Pakrasi 1993). Further studies of PsbL mutants from tobacco has showned that this plants are unable to grow photoautotrophically, and if sucrose was added they only grew slowly with pale green leaves: no photosynthetic activity was detected in them. According to these studies we can conclude that PsbL is essential for the normal function of PSII. Its deletion causes fatal damage to PSII in both cyanobacteria and tobacco plants, especially for donor side electron transfer, PSII core assembly and maintenance of the dimeric form of PSII.

PsbM

The PsbM (chloroplast encoded) contains 31-38 amino acid residues, with calculated molecular masses between 3.5 and 4.2 kDa. Sequence analysis suggests that the PsbM protein is one of the most hydrophobic proteins in the thylakoid membrane. The PsbM protein from Arabidopsis shares 54% identity to that from Synechocystis 6803. The PsbM protein has been detected in PSII complexes isolated from Cyanobacteria and higher plants in particular from pea using proteomic techniques. It is

located with PsbL and PsbTc at the monomer–monomer interface of the dimeric core complex and it contribute to the stabilization of PSII dimers (Ferreira et al. 2004). PsbM is not the only protein responsible for dimer stabilization in fact knock-out of psbM in tobacco plants revealed that PsbM is not required for biogenesis of higher order PSII complexes in plants, but it alters the properties of the Q B site and the electron flow within PSII (Umate et al. 2007).

PsbN

The PsbN protein contains 43 amino acids and has a molecular mass of 4.5-5.0 kDa in most species. The effects of deleting both PsbN and PsbH on PSII activity in Synechocystis 6803 were the same as those of solely deleting the PsbH protein, indicating that PsbN is not essential for photoautotrophic growth and normal PSII function. PsbN protein has not been detected directly in plant PSII, and it is not present in the crystal structures of PSII isolated from cyanobacteria. The only evidence of its presence in a PSII preparation from the cyanobacterium Synechococcus vulcanus (Ikeuchi et al. 1989a) was reexamined by Kashino and colleagues (Kashino et al. 2002), who revealed that the protein originally regarded as PsbN in that preparation was actually PsbTc. These results strongly suggest that PsbN is not a PSII protein.

PsbR

The PsbR protein also named the 10-kDa polypeptide (with a molecular mass of 10.3 kDa) contains 99 amino acids. Studies have indicated that PsbR could not be removed from the membrane by treatment with high salt concentrations. Ou Infact predictions indicate that it contains a transmembrane span close to its C-terminus and during purifications PsbR presents hydrophobic property (Ljungberg et al. 1986; Lautner et al. 1988). Recent studies have shown that PsbR has a charged domain. These particular features suggest that PsbR is a docking protein, in particular it has been proposed that PsbR has a binding site for the extrinsic PsbP protein. Nevertheless, it has been also found that when PsbS and PsbR proteins were removed from PSII, the extrinsic PsbO, PsbP and PsbQ proteins were retained suggesting that not only PsbR is involved in the docking of the PsbP protein. Further studies on the function of PsbR have demonstrade that the PsbR mRNA is accumulate upon light exposure and the PsbR protein was undetectable in etiolated spinach, in contrast to the expression patterns of the PsbO, PsbP and PsbQ extrinsic proteins (Lautner et al. 1988).

PsbS

The PsbS protein is not part of LMM subunits in fact it has 205 amino acids and a molecular mass of 22 kDa. This subunit is nuclear encoded and it has been predicted to have four transmembrane helices. PsbS protein has a high sequence homology with the light-harvesting proteins of the Lhc family (Funk et al. 1995), buti t has a transmembrane helix more and for its still controversial ability in the native form to bind Chl and carotenoid molecules (Funk et al. 1995; Dominici et al. 2002). Recent studies have shown that PsbS is able to bind exogenous zeaxanthin (Aspinall-O'Dea et al. 2002). This binding may be associated with the formation of nonphotochemical quenching centres of Chl fluorescence (qE) functioning to dissipate excess light energy absorbed by PSII lightharvesting system, a phenomenon in which PsbS is known to play a crucial role (Li et al. 2000). Recently, an explanation for this role has been provided showing that PsbS controls the macro-organization of the grana membranes in higher plant chloroplasts. The regulation of PsbS interaction between the antennae and the PSII core in the thylakoid membranes of higher plants seems to be via pH induced conformational changes (Kiss et al. 2008). As it was difficult to locate PsbS to any particular place in membrane fractionation studies, it was suggested that it is mobile in the thylakoid membrane (Teardo et al. 2007) and that its location can be determined by a reversible dimerization (Bergantino et al. 2003).

PsbTc and PsbTn

The psbTc gene is highly conserved among cyanobacteria, algae and higher plants. The lower case c in the name of this protein indicates that in higher plants and algae the protein is chloroplast-encoded. The product of this gene contains 31-38 amino acids with molecular masses ranging from 3.5 to 4.4 kDa. PsbTc is an intrinsic protein with a single transmembrane helix close to the N-terminus. PsbTc has been detected in C. reinhardtii and spinach. It has been proposed that the C-terminal tail of the protein is exposed to the stromal side of the thylakoid membrane. The predicted orientation of PsbTc, as well as PsbK, is similar to that of nuclear-encoded PsbW and PsbX, but opposite to that of other small, chloroplastencoded PSII proteins. PsbTc has been proposed to have an intimate association with the D1 and D2 proteins (Zheleva et al. 1998). The function of this subunit has been studied in a deletion mutant from C. reinhardtii where the growth and PSII function were impaired under high light conditions. Therefore, it has been suggested that the protein is required for maintaining optimal PSII activity under adverse conditions, such as high light stress. Further studies revealed that this chloroplast-encoded protein undergoes degradation upon high light, but does not play a role in photoprotection. Instead, it is required for efficient recovery of photodamaged PSII. It has been

proposed that PsbTc in C. reinhardtii is involved in posttranslational events during photoinhibition. (Monod et al. 1994, Ohnishi and Takahashi 2001).

PsbTn (nuclear encoded protein) has been purified and partially sequenced from PSII core complexes of spinach and wheat, it is a hydrophilic protein with an apparent molecular mass of 5.0 kDa according to polyacrylamide gel analyses, and was previously named the 5.0-kDa. After the maturation process , the protein has only 28 amino acids and a molecular mass of 3.2 kDa in Arabidopsis, making it the smallest known polypeptide in the PSII complex to date. The function of PsbTn protein is unknown but there is a bipartite presequence in its amino acid sequence characteristic of the lumenal proteins, so it has been suggested that the protein could be an extrinsic protein.

PsbW

The nuclear psbW gene is present in green algae and in higher plants. This gene encodes a protein (PsbW) with a long transit peptide (59-83) amino acid residues in length depending on species) .The mature PsbW protein, previously known as the 6.1-kDa protein, is composed of 54 amino acid residues in spinach and Arabidopsis. The PsbW protein has one transmembrane span and the N-terminus of the protein was demonstrated to be located on the lumenal side and the C-terminus on the stromal side of the thylakoid membrane. The PsbW protein is tightly associated with the PSII reaction very close to the large subunit of Cyt b 559. Expression of the PsbW gene is light-regulated at both mRNA and protein levels in Arabidopsis, in fact study on photoinhibition demonstrated that the repair of photoinhibitory damaged PSII involves the rapid turnover of the PsbW protein. Recent studies have showned that in knock-out Arabidopsis mutants the supramolecular organization of PSII–LHCII supercomplexes is widely compromise, suggesting a more peripheral positioning close to the minor antenna complexes in PSII (García-Cerdán et al. 2011).

PsbX

The PsbX protein is nuclear-encoded in higher plants and in some algae where it is located in the chloroplast or cyanelle. PsbX precursor from Arabidopsis has a bipartite presequence of 74 amino acid residues, which is absent in its plastid-encoded counterpart in algae. This evidence could suggests that the gene has been transferred from the plastid to the nucleus and acquired the transit peptide (Kim et al. 1996). The mature PsbX protein contains 38-42 amino acid residues with a calculated molecular mass of 4.0-4.2 kDa, depending on the organism. Predictions according to its primary sequence indicate that PsbX has a single transmembrane span and that the N-terminus is located at the lumenal side of the

membrane. The higher plant PsbX is located within the PSII core, but it was undetectable in either PSIIRC or LHCII preparations. Recent studies has been swooned that the expression of the psbX gene is light-regulated at both the mRNA and protein levels in Arabidopsis. The regulation of psbX mRNA in Synechocystis 6803 instead, under normal light conditions has been found to be independent of light, although it is expressed strongly during high light treatment. Inactivation of the psbX gene in Synechocystis 6803 caused a reduction in the amount of PSII and a slight uncoupling of the antenna. In the psbX deletion mutant the donor and acceptor sides of PSII functioned properly under normal and stress conditions (such as high light, and salt stress) but the decrease of the PSII amount might suggest that the PsbX protein are directly or indirectly involved in regulation of the amount of PSII (Shi et al. 1999, Funk 2000).

PsbY

The psbY gene in higher plant encodes a much larger polypeptide precursor (19.5 kDa in Arabidopsis and 20.7 kDa in spinach). The precursor is synthesized in the cytosol, imported into the chloroplast, then subjected to several steps of processing and maturation to generate two thylakoid membrane proteins, PsbY-1 and PsbY-2 with molecular masses of 4.7 and 4.9 kDa respectively. In Arabidopsis, both PsbY proteins have been predicted to have one transmembrane span with the N-terminus at the lumenal side of the thylakoid membrane. The twin PsbY proteins have been isolated from spinach PSII membrane fractions (BBY particles). Further studies have reported that the PsbY protein have catalase-like manganese-dependent activity and an L-arginine metabolizing activity that converts L-arginine into ornithine and urea (Gau et al. 1998).

PsbY mRNA was found in leaves, but not roots, stems or etiolated materials. The amount of mRNA increased during the first couple of hours of illumination, and then decreased.

Deletion mutagenesis in Synechocystis 6803 has showned that the psbY mutant cells have normal photosynthetic activity and that PsbY protein does not play an essential role in the photosynthetic water oxidation process, in accordance with its localization in the periphery of PSII, far from the OEC (Meetam et al. 1999). A discrete function for this subunit is still unknown, and a higher plant psbY knockout mutant is needed.

PsbZ

The PsbZ protein is encoded by a chloroplast gene, psbZ, highly conserved among organisms, contains 62 amino acid residues and its theoretical molecular mass, in Arabidopsis is 6.6 kDa. PsbZ has been co-

purified with LHCII complexes from tobacco plants. Thus, it has been suggested that the location of this protein seems to be at the interface of PSII and LHCII complexes. Recent studies have pointed out in evidence that psbZ knockout tobacco plants developed pale leaves under standard heterotrophic growth conditions due to a reduction in chlorophyll content; the plants also have shown a dwarf phenotype in low light conditions. Moreover the level of the antenna proteins CP26 and CP29 were found to be markedly reduced in psbZ knockout plants. The lack of the PsbZ protein and the consequently decrease of the amounts of CP26 and CP29 caused structural changes in PSII that prevented the isolation or detection of PSII–LHCII supercomplexes in electron microscopy studies. (Swiatek et al. 2001).

However, as the loss of PsbZ leads to reduced amounts of CP26, these effects may be secondary. To summarize, PsbZ is likely to be a structural factor that stabilizes PSII–LHCII supercomplexes. It may also be involved in photoprotective processes under suboptimal growth conditions. In cyanobacteria, where the light-harvesting system is completely different from higher plants, a role for PsbZ in the regulation of electron transfer activity through the two photosystems with implication in photoprotection has been suggested (Bishop et al. 2007).

Oxygen evolving extrinsic subunits:

The catalythic site of higher plants PSII, which is also known as OEC, is composed by a Ca-Mn cluster and three extrinsic subunits namely PsbO, PsbP and PsbQ.

The OEC proteins are nuclear-encoded but PsbP and PsbQ are present only in higher plants and in green algae. In cyanobacteria and in red algae they are substituted by PsbU and PsbV although there are some differences in the function and binding properties. Concidering recently study, wich have been found in the cyanobacterial PsbQ and PsbP homologues, it has been proposed that the ancestor of the oxygenic photosynthetic organism had all the extrinsic proteins (Roose et al. 2007; Enami et al. 2005; Ishihara et al. 2007). At the present state, after several years of evolution, Enami and their coworkers, individuate three evolutionary branch: and green algae and higher plants, which have PsbO, PsbP and PsbQ; Red algae and Diatoms, which have PsbO, PsbQ homologous (in stoichiometric amount) PsbU and PsbV and Cyanobacteria, which have PsbO, PsbU and PsbV.

This phylogenetic division reflect their adaptation to different ecological niches, in fact type and Chl content changes through these three groups. Another evidence of the evolution of PsbP from the ancestor to primitive green algae and higher plants it has been found in two PsbP-like proteins (PPL1 and PPL2) in the lumen of Arabidopsis (Ishihara et al. 2007). As it has been said before, all these

proteins in eukaryotes have their coding region in the nuclear genome, Ishihara and their co-workers claim that probably the gene transfer from the chloroplast genome to the nuclear in order to allow a greater diversification of the gene product structures and functions.

The expression of the OEC genes is finely regulated and in fact, it has been found that, in the extreme halophyte *Salicornia veneta*, the psbQ and psbP genes are strongly underexpressed (Pagliano et al. 2009). Thus, some PSII subunits, like OEC proteins, could be involved in an evolutional adaptation to an extreme ecological niche.

PsbO

PsbO protein also called 33 kDa Manganese Stabilizing Protein is a component of the PSII OEC in every type of oxygenic photosynthetic organism. Biochemical and genetic studies have shown that the PsbO protein play a crucial structural and functional role in many different types of OECs. The most important functions carried out by PsbO are: stabilize the manganese cluster and modulate the Ca^{2+} and Cl^- requirements for oxygen evolution (Bricker, 1992).

This extrinsic subunit is conserved from cyanobacteria to higher plants, where it is nuclear-encoded. PsbO protein is often referred to as the 33 kDa protein, but after processing it has a calculated molecular mass of 26.5 kDa and its sequences is composed by 240-257 residues, depending on species. The crystal structure of this protein shows an elongated shape with two main domains: a β-barrel structure composed of eight antiparallel β-strands and an other domain, formed by a loop joining β-strands 5 and 6. The β-barrel plays an important role in stabilizing the manganese cluster and in maintaining an optimal environment for water oxidation (De Las Rivas and Barber, 2004). Other studies have been shown that PsbO mantain the optimal Ca^{2+} and Cl^- levels at the catalytic site, but it does not bind Mn directly.(Briker et al. 2008). The loop binds to the lumenal surfaces of the D1, D2, CP43 and CP47 proteins. The deletion of the psbO gene in cyanobacteria did not prevent water oxidation, although increased susceptibility to photoinhibition was observed (Philbrick et al. 1991; Mayes et al. 1991). In Arabidopsis there are two PsbO proteins called PsbO1 and PsbO2. They differ only by 10 amino acids in their mature form and also for their expression, in fact PsbO1 isoform is four- to fivefold more abundant than PsbO2 (Murakami et al. 2002). An Arabidopsis mutant with an impaired psbO1 gene shown retarded growth, although the level of the PsbO2 protein was significantly increased (Murakami et al. 2002, 2005). Two T-DNA insertion mutant lines of Arabidopsis deficient in either the PsbO1 or the PsbO2 protein has helped to understand the different functions of the two

isoforms: PsbO1 seems to mainly support PSII activity, whereas the interaction of PsbO2 with PSII regulates the turnover of the D1 protein, increasing its accessibility to the phosphatases and proteases involved in its degradation, a mechanism possibly mediated by its GTP hydrolytic activity (Lundin et al. 2007, 2008).

The absence of the PsbO protein has varying effects on PSII depending on the organism. For example, plants, not in alla cases, and the green alga *Chlamydomonas reinhardtii* are not capable of photoautotrophic growth without PsbO (Mayfield et al. 1987; Yi et al. 2005). Cyanobacterial PsbO mutants can grow photoautotrophically, although at lower levels relative to wild type (Philbrick et al. 1991). One of the major controversy associated with PsbO, involves its stoichiometry within the PSII complex. Structural analyses of cyanobacterial PSII indicate one PsbO per PSII monomer (Kamiya and Shen 2003; Ferreira et al. 2004; Loll et al. 2005), but reconstitution studies in plants indicate the molar ratio of PsbO in PSII is two (Bricker, 1992; Popelkova et al. 2002b). This data can be reconciled by the recent observation that plant PsbO contains two sequence motifs at its N-terminus which determine binding stoichiometry, while cyanobacterial PsbO has only one such sequence (Popelkova et al. 2002a). However, structural studies of plant PSII show there is not sufficient electron density to accommodate two copies of the PsbO protein (Nield et al. 2002; Nield and Barber, 2006).

PsbP

The PsbP protein (also called 23 or 24 kDa protein) was first determined to be a component of PSII in plants, but psbP gene can even be found in the primitive cyanobacterium *Gloeobacter violaceus* which lacks thylakoids, suggesting an ancient role for this protein in PSII. Arabidopsis has 10 copies of the psbP gene in its genome and eight of these were found to be expressed proteins in the thylakoid lumen (Schubert et al. 2002). PsbP was first identified during release–reconstitution experiments in higher plants. The PsbP and PsbQ proteins are removed by 1 M NaCl treatment with a concomitant decrease in oxygen evolution. Addition of Ca^{2+} and Cl^{-} to the assay medium restores PSII activity without the addition of these proteins (Ghanotakis et al. 1984; Miyao and Murata, 1985). Specifically, PsbP was found to modulate the Ca^{2+} requirement for PSII activity and has been hypothesized to act as a Ca^{2+} concentrator and prevent release of Ca^{2+} during turnover of PSII (Miyao and Murata, 1984). Multiple studies have shown that PsbP has implicated, with PsbQ, also in the regulation of the Cl^{-} requirement. Clearly the PsbP protein functions to modulate the ionic requirements for oxygen evolution, but it also plays a structural role to protect the manganese cluster from attack by exogenous reductants (Ghanotakis et al. 1984). Altought PsbP and PsbQ proteins are extremely important in the ionic

recruitment, recent studies have shown that in the extreme halophyte *Salicornia veneta* the psbQ and psbP genes are strongly underexpressed but the oxygen evolving activity is not compromised (Pagliano et al. 2009).

In mutagenesis studies, plants lacks the PsbP protein, accumulates PSII centers, high concentrations of Cl^- were necessary to promote oxygen evolution and there were significant defects in the light-driven assembly of the manganese cluster . This inefficient photoactivation process and decreased Cl^- affinity resulted in a substantial amount of competing donor side damage. These data suggest a specific role for PsbP in the functional assembly of the manganese cluster and stability of PSII.

The PsbP knock-down plants exhibited a reduced variable fluorescence yield, lower oxygen evolution and decreased amounts of PsbQ, which has been shown to require PsbP for binding to PSII in plants. RNAi studies shown that all of the isoforms are required for optimal activity, but generally PSII activity was correlated with the total amount of PsbP protein. Therefore the PsbP protein is essential for normal in vivo PSII activity in plants because it is critical for OEC stabilization. (Ishihara et al. 2005). The essential role of PsbP for normal thylakoid architecture was further emphasized in Arabidopsis mutants, where dramatic alterations in thylakoid structure were found in plants expressing low and intermediate amounts of the PsbP protein under normal growth light conditions (Yi et al. 2009). Similar results were obtained in tobacco mutants, where the knockdown of PsbP impaired also the accumulation of PSII supercomplexes (Ido et al. 2009).

Thornton and his co-workers have determined amount of PsbP by using quantitative immunoblot comparisons of the proteins relative to antigen standards and it seems to be approximately 3% of that of CP47 in the thylakoid membranes. In plants, binding of the PsbP protein requires PsbO and is hypothesized to be a largely electrostatic interaction (reviewed in Seidler, 1996). In contrast, PsbP from green algae has been shown to bind independently of the other extrinsic proteins (Suzuki et al. 2003). These variations in the binding properties of PsbP highlight structural adaptations for associating with distinct combinations of proteins in the OECs of different organisms. Refer to the sections for the organismspecific OECs for further discussion. Currently, a high resolution (1.6 Å) crystal structure of PsbP from Nicotiana is available (Ifuku et al. 2004). The crystal structure of PsbP has revealed that the core is an anti-parallel β-sheet with α-helices on either side (Figure 1.5).The electron densities of the N-terminal 15 residues, and two loop regions were not resolved.

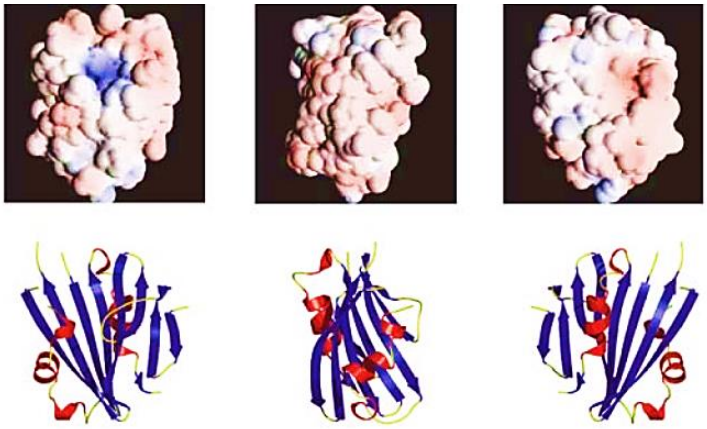

Figure 1.5. PsbP crystal structure at 1.6 Å (Ifuku et. al 2004).

This result may indicate possible stabilizing conformational changes in PsbP upon binding. Further studies on PsbP N-terminus indicate that this portion of the protein is critical for ion retention in PSII (Ifuku and Sato 2001), but it hasn't been reported any mechanism for its function. PsbP structure suggest a non-conventional role of the protein in plant PSII; in fact PsbP is very similar to that of Mog1p, a regulatory protein for a Ran GTPase suggesting it may be a possible GTP/GDPsensitive regulator (Ifuku et al. 2004; De Las Rivas and Roman, 2005).

PsbQ

The psbQ genes have been identified in a number of different photosynthetic organisms. Arabidopsis contains multiple copies of psbQ genes, four of which have been identified as expressed proteins in the thylakoid lumen (Peltier et al. 2002; Schubert et al. 2002). Arabidopsis contains two expressed PsbQ proteins (Peltier et al. 2000; Schubert et al. 2002), encoded by two genes, psbQ-1 and psbQ-2.

The protein PsbQ (known also as 16-18 kDa protein), in its mature form, contains 149 amino acids and has a molecular mass of 16.5 kDa. Like PsbP, it is located close to PsbO and the Mn_4CaO_5 cluster of the OEC in higher plants and green algae, where it is nuclearencoded. Its gene has been found in a number of different photosynthetic organisms including cyanobacteria, where this subunit (known as PsbQ-like protein) can be stoichiometric with PSII (Thornton et al. 2004) and isolated as such (Roose et al. 2007b).

High-resolution crystal structures of isolated spinach PsbQ protein (Calderone et al. 2003; Balsera et al. 2005) have revealed that the PsbQ protein can be divided into two structural domains: a C-terminal four-helix bundle with an asymmetric charge distribution and a flexible N-terminus. The PsbQ N-

terminal region include two short b-strands surrounding a large flexible loop region (residues 14-33) and a polyproline type II motif (Balsera et al. 2005), which may obtain a more rigid conformation upon binding PSII.

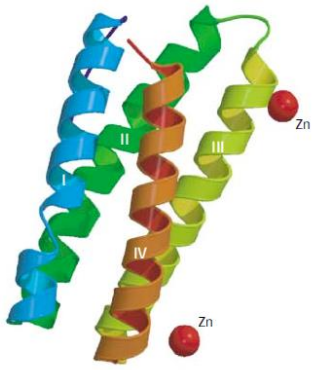

Figure 1.6. PsbQ crystal structure at 1.95 Å (Calderone et al. 2003).

The crystal structures of PsbQ show two bound Zn^{2+} atoms, where the coordinating residues of one atom are entirely conserved in the plant PsbQ proteins (Calderone et al. 2003; Balsera et al. 2005). While Zn^{2+} was specifically required for crystal growth, the biological significance of this result has yet to be determined.

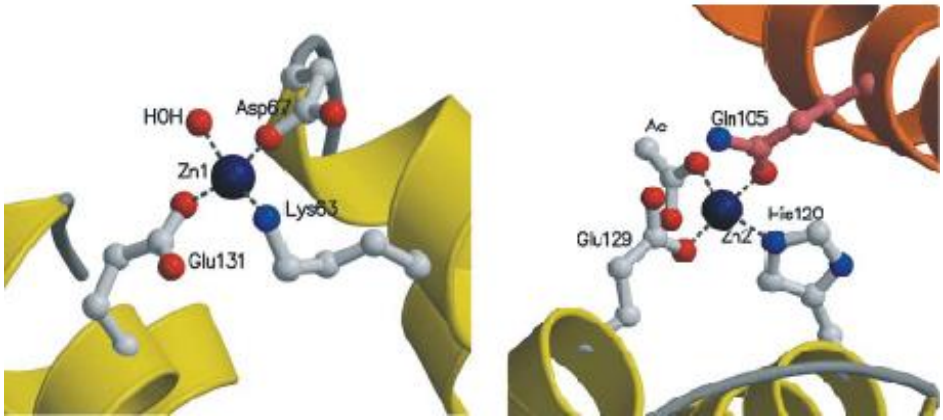

Figure 1.7. Zn^{2+} binding domain of the PsbQ crystal structure (Balsera et al. 2005).

The cumulative data on PsbQ indicate it is a key structural component of OECs from a number of different organisms, but many questions remain regarding its function and its mode of association with PSII. High-resolution structures of PSII complexes containing PsbQ are necessary to provide insights

into its role in the ionic requirement for oxygen evolution and its location relative to the other protein components of the OEC.

In higher plants, the binding of PsbQ to PSII requires the presence of PsbO and PsbP (reviewed in Enami et al. 2008). Biochemical in vitro studies have shown that PsbQ, like PsbO and PsbP, is involved in modulating the Ca^{2+} and Cl^- level for optimal oxygen evolution activity (reviewed in Seidler 1996; Roose et al. 2007a; Bricker et al. 2012). In particular, PsbQ, in concert with PsbP, functions to lower the Cl- requirement for optimal activity. (Ghanotakis et al. 1984; Miyao and Murata, 1985). This finding fits well with the evidence that in some halophytic plants, growing in extremely salty environments, the presence of PsbQ is dispensable (Pagliano et al. 2009; Trotta et al. 2012).

1.2.3 Light Harvesting Complex and PSII Ultrastructure (PSII-LHCII supercomplex)

Light harvesting complex II

In photosynthetic organisms PSII core dimer is serviced by a number of extra chlorophyll binding proteins which transfer the excitation energy to CP43 and CP47. The number and type of this supplementary antennae complexes vary among the different types of oxygenic photosynthetic organisms. To efficiently harvest the available spectrum of light energy that drives photosynthesis, different photosynthetic organisms use diverse proteins, each one binding specific pigment molecules. In cyanobacteria and eukaryotic red algae, light harvesting for PSII is carried out primarily by a group of pigmented proteins, called phycobiliproteins, encoded by apc and cpc genes that become constituents of the extrinsic macromolecular complex called phycobilisome (PBS).

In higher plants the polypeptides which bind the pigments are called Chl a/b binding proteins (also known as Cab or Lhcb proteins). They are part of the Lhc gene super family which consists of the lhcb1, lhcb2, lhcb3, lhcb4 (CP29), lhcb5 (CP26) and lhcb6 (CP24) genes products are collectively called LHCII (Jansson, 1999; Dekker and Boekema, 2005). Lhcb1, Lhcb2, and Lhcb3 are associated with various combinations in order to form trimeric structures, while CP29, CP26 and CP24 are monomers which are closely associated with PSII. The number of associated Lhcb trimers differs as a consequence of the light growing conditions and among the different species (Jackowski et al. 2003). They have been resolved the crystal structure of the LHCII trimer at 2.7 Å (Liu et al. 2004) and the monomeric Lhcb protein CP29 at 2.8 Å (Pan et al. 2011). These crystal structures have revealed that all the Lhcb polypeptides span the membrane by means of three highly conserved α helices. Furthermore, they bind various chlorophyll b molecules, besides chlorophyll a molecules and xanthophylls and β

carotene. It has been calculated that 200-300 pigment molecules are associated with LHCII along with CP43 and CP47 per PSII monomer (Barber, 2006). The LHCII proteins are important not only for the light harvesting activity, but also for the protective role under high light intensity too. The core complex has to be protected from excess light. This is mainly achieved by the harmless dissipation of the excitation energy into heat by a process that is known as high- energy quenching (qE), a component of the NPQ. The process is triggered by acidification of the thylakoid lumen, which activates violaxanthin de-epoxidase (VDE), which, in turn, converts violaxanthin into zeaxanthin; PsbS is also involved in this process. It is worth noting that the Lhcb proteins bind 78% of the total violoxanthin associated with the PSII antenna system. The trimeric LHCII complexes are present also in the green alga C. reinhardtii, where the polypeptide components are encoded by 9 lhcbm genes (Lhcbm1-6, Lhcbm8, Lhcbm9 and Lhcbm11). In addition, green algae contain also the monomeric polypeptides Lhcb4 and Lhcb5, but not Lhcb6.

PSII-LHCII supercomplexes

In higher plants, in stacked grana region, PSII is organized in PSII-LHCII Supercomplex which are composed by a dimeric core complex of PSII (C_2), which is associated with two copies of each minor light-harvesting protein CP26 and CP29, strongly bound two LHCII trimers called trimer S. (Boekema et al. 2000; Yakushevska et al. 2001; Dekker and Boekema, 2005). This PSII-LHCI supercomplex called C2S2 contains almost all PSII core proteins but the peripheral antenna the Lhcb3 and CP24 proteins appear to be absent. A threedimensional structure of this supercomplex from spinach was constructed using a low-resolution 3D electron density map obtained by single particle cryo electron microscopy (Nield and Barber et al. 2006). They have been found larger PSII-LHCII supercomplexes, containing two extra copies of the monomeric Lhcb6 with two additional LHCII trimers (M-trimer) moderately bound to the C_2 via Lhcb4 and Lhcb6, are known as $C_2S_2M_2$. Occasionally, they have been also observed in isolated spinach thylakoids fragments, supercomplexes with one or two additional LHCII trimers (L-trimer) loosely bound to the dimeric PSII core dimer. These supercomplexes have been called $C_2S_2M_2L_{1-2}$ (Boekema et al. 1999). PSII-LHCII supercomplexes have been isolated with α-DM and β-DM mild treatment, from thylakoids or PSII membranes (BBY). They have been isolateddirectly from thylakoids, a variety of different-sized PSII-LHCII structures, including the $C_2S_2M_2$ and C_2S_2 supercomplexes. (Bumba et al. 2004 and Eshaghi et al. 1999). Recently, by using α-DM to solubilize BBY preparations from wild-type and LHC mutants of Arabidopsis they have been

obtained a wide range of PSII–LHCII supercomplexes separated by sucrose density centrifugation. $C_2S_2M_2$ supercomplex of Arabidopsis thaliana and shows details at 12 Å resolution (Caffarri et al. 2009), permitting a more accurate fitting of the peripheral antenna proteins, based on the known LHCII structure. The combination of high-resolution structures of components with the low-resolution provided by electron microscopy is useful because the precision of fitting an X-ray structure into an EM density map is much better than the resolution of the EM data (Rossmann et al. 2000).The model proposed shows how within the PSII–LHCII supercomplex the innermost LHCII S-trimer is attached to a dimeric PSII via CP29, binding to one PSII core monomer and CP26 to the other.

PSII–LHCII supercomplexes with empty Lhcb4 binding sites could be found and this suggests that CP29 occupies a unique position in the PSII macrostructure and that in contrast to CP26 its presence is essential for the formation of PSII–LHCII supercomplexes. Both the CP29 and CP26 antisense mutants shown a rather normal photosynthetic performance, although the mutants shown slightly different fluorescence characteristics and an increased number of PSII centers (Andersson et al 2001). As mentioned before, CP24 is necessary for binding the M-trimer in fact Arabidopsis plants and the green alga Chlamydomonas reinhardtii depleted of CP24 do not form $C_2S_2M_2$ supercomplexes (Kovacs et al. 2006). Recent studies conducted on supercomplexes isolated from Arabidopsis plants expressing an antisense construct to Lhcb2 have revealed that the expression of the antisense Lhcb2 construct resulted in strongly increased levels of CP26 and Lhcb3, and that supercomplexes were formed with trimers consisting of Lhcb5 and Lhcb3 at the S- and M-binding positions (Ruban et al. 2003).

PSII-LHCII supercomplexes are localized in stacked grana membranes and their distribution is different. Most grana membranes show a rather random organization, but in some conditions, which are still not exactly understood, large parts of the membranes occur in semi-crystalline domains and row-like associations. The formation of semi-crystalline domains in the membrane requires a physical separation of PSII supercomplexes from the other membrane proteins. Crystalline 2D arrays of dimeric PSII have been observed decades ago after freeze-etching and freeze-breaking of green plant photosynthetic membranes There is quite some variation in these crystalline arrays, which depends on factors like temperature and biochemical composition of the grana membranes. At least three types of supercomplexes can form the crystals C_2S_2, C_2S_2M and $C_2S_2M_2$ moreover, these different types of particles can arrange in several different types of packing, which means that the interaction with neighbors is different (Kirchhoff et al. 2007).

1.3 Detergents and thylakoids solubilization.

The use of detergents to solubilize thylakoid membrane it is the first step in the isolation of the membrane protein complexes membranes to study their native structural and functional properties. For an efficient solubilization, it is necessary to study first the membrane characteristics, the nature of the proteins and also the chemical properties of the detergent used. Thylakoid membranes show a unique lypidic composition compared with other biological membranes. There is a high proportions of the glycolipids monogalactosyldiacylglycerol (MGDG), digalactosyldiacylglycerol (DGDG), and sulfoquinovosyldiacylglycerol (SQDG). The protein complexes embedded in the thylakoid membranes, described above, have a complex pattern of hydrophobic interactions with the membranes lipid bilayer. The amount of detergent must to be higher than the critical micelle concentration (CMC) to induce the solubilization. In fact, when the concentration of detergent achieve the CMC, the detergent molecules self associate in micelles and the solubilization begins. It has been shown that the activity/intactness of solubilized protein complexes is dependent on the co-extraction of lipids with the proteins therefore it is important not to over solubilize the thylakoid membranes in order to maintain the protein structure bintact (De Grip et al. 1982). Detergents have been classiefied in four different groups; they are: the ionic detergents, the non-ionic detergents, bile acid salts, and zwitterionic detergents. The most commonly used in the solubilization of thylakoid membranes are the non-ionic surfactants such as the alkylglucosides. Of this, there are the so called "mild" detergents that mainly break lipid–lipid and lipid–protein interactions leaving the structure of the isolated protein intact. In the table 1 are reported the most common mild detergents. Detergents with longer alkyl chain are generally milder than the ones with short alkyl chains and also, the larger the head group the milder the detergent (Deisenhofer et al. 1985, Sardet et al. 1976). However, short chain (C7-C10) nonionic detergents, such as n-octyl-h-d-glucopyranoside (OG), can often lead to deactivation of the protein, unlike their corresponding intermediate (C12 –C14) chain derivatives (Lund et al 1989). One of the most important mild detergent is Dodecylmaltoside (DM). DM have an extremely large and rather stiff hydrophilic head group made up of two sugar rings (maltose) and a noncharged alkyl glycoside chain (C12). There are two isomers of this molecule: α-DM and β-DM, which have significant differences in molecular architecture, because the alkyl chain is in axial orientation in α-DM while in β-DM is in equatorial orientation respect to the headgroup. These different molecular architecture has a strong impact on the chemical properties of both isomers as you can see in figure the CMC is higher in β-DM than in α-DM, the micellar shape is spherical in α-DM and oblate ellipsoid in β-DM and the micellar radius value and the

aggregation number is higher in β-DM than α-DM (Cecutti et al. 1991; Bäverbäck et al. 2009). Both DM isomers have been widely used in thylakoid solubilization in particular β-DM is used in: isolation from higher plants thylakoids of integral multi-subunits photosynthetic complexes, and in crystallization procedures. α-DM, instead, it has been used to solubilize plant thylakoid membranes in a single step treatment, obtaining intact grana or fully solubilized PSI and PSII complexes.

Tissue source	Membrane protein/glycoprotein	Surfactants used	Reference
Purple membrane *Halobacterium halobium*	Bacteriorhodopsin	Triton X-100	Lévy et al., 1990 Rigaud et al., 1988
Bacillus lichenformis	Penicillinase	OBG	Helenius et al., 1981
Trypanosoma brucei	D-Glucose transporter	OBG, octylthioglucoside	Seyfang and Duszenko, 1993
Torpedo californica	Acetylcholine receptor	Sodium cholate	Jones et al., 1987a
Semliki forest virus	Spike glycoprotein	OBG	Helenius et al., 1981
Vesicular stomatitus viruses	G and M envelope protein	OBG	Paternostre et al., 1997
M13 bacteriophage	Coat protein	Sodium cholate	Florine and Feigenson, 1987
Spinach chloroplasts	H^+-ATPase	Triton X-100	Lévy et al., 1990 Richard et al., 1990
Spinach chloroplasts	Photosystem II	OBG, *n*-dodecyl-β-D-maltoside	Hankamer et al., 1997
Pea photosynthetic system	Chlorophyll *a*/*b* light harvesting complex	Triton X-100	McDonnel and Donner, 1981
Zucchini (zea) plasma membrane	Auxin-binding protein	Triton X-114	Hicks et al., 1993
Castor oil seeds endosperm	Acid lipase	CHAPS	Fuchs et al., 1996 Altaf et al., 1997
Vero cell plasma membrane	Kunjin virus receptor	OBG	Sankaran et al., 1997
Ricinus cotyledons	H^+-ATPase, H^+-PPase	*n*-Dodecyl-β-D-maltoside	Long et al., 1997

Table 1.1 Most common mild detergents (Jones, 1999).

GENERAL MATERIALS AND METHODS

2. GENERAL MATERIALS AND METHODS:

2.1 Plants growth

Before sowing, pea (*Pisum sativum* L., var. Palladio nano) seeds were treated as described in (Pagliano et al. 2006). Germinated seedlings were transferred to pots and grown hydroponically in Long Ashton nutrient solution in a growth chamber with 8 h daylight, 20 °C, 60% humidity and 150 µmol m-2 s-1 photons. Leaves from plants grown for 3 weeks were harvested and used for experiments.

2.2. Isolation of thylakoid membranes

Thylakoid membranes were isolated with divalent cations Mg^{2+} in order to mantain the appressed grana region. Briefly, pea leaves were disrupted by grinding with a blender in 50 mM HEPES pH 7.5, 300 mM sucrose and 5 mM $MgCl_2$. The suspension was passed through a filter and the filtrate was centrifuged at 1500×g for 10 min. The pellet was washed once by centrifugation in the same buffer and then homogenized in 5 mM $MgCl_2$ and diluted 1:1 with 50 mM MES pH 6.0, 400 mM sucrose, 15 mM NaCl and 5 mM $MgCl_2$ followed by 10 min centrifugation at 3000 ×g. The resulting pellet of thylakoid membranes was washed once by centrifugation in 25 mM MES pH 6.0, 10 mM NaCl and 5 mM $MgCl_2$. Thylakoid membranes were suspended and stored in 25 mM MES pH 6.0, 10 mM NaCl, 5 mM $MgCl_2$ and 2 M glycine betaine (MNMβ buffer).

2.3. Thylakoids solubilization with α-DM and β-DM

Equal amounts of stacked thylakoid membranes were suspended in MNMβ buffer and solubilized at a Chl concentration of 1 mg/ ml with different concentrations (ranging from 5 to 100 mM) of α-DM or β-DM in the dark on ice for 1 min. Non-solubilized material was then removed by double centrifugation at 21,000 ×g for 10 min at 4° C. For each concentration of detergent, membrane pellets were resuspended in MNMβ buffer and, together with their corresponding supernatants, quantified on a Chl basis. Finally the percentage of solubilization for each detergent treatment was calculated as the ratio between the amount of Chl in the supernatant over the total amount of Chl of thylakoids treated with the detergent.

2.4 Isolation of PSII–LHCII supercomplexes

Thylakoid membranes having a Chl concentration of 1 mg ml in MNMβ buffer were treated with 50 mM α-DM or β-DM for 1 min at 4°C in the dark. Phenylmethylsulphonylfluoride (500 mM) was present during the solubilization to inhibit protease activity. After a short centrifugation at 21 000g for 10 min at 4° C, 700 ml of the supernatants was added to the top of linear sucrose gradients, prepared by freezing and thawing ultracentrifuge tubes filled with a buffer made of 0.65 M sucrose, 25 mM MES pH 5.7, 10 mM NaCl, 5 mM $CaCl_2$ and 0.03% α-DM or β-DM. Centrifugation was carried out at 100 000g for 12 h at 4° C (Surespin 630 rotor, Thermo Scientific). Sucrose bands, containing PSII- LHCII particles, were carefully removed using a syringe and, if necessary, concentrated by membrane filtration with Amicon Ultra 100 kDa cut-off devices (Millipore) and then stored at -80° C.

2.5. Spectroscopic measurement

Absorption spectra for solubilized thylakoids and for both isolated supercomplexes were recorded using a Lambda25 spectrophotometer Perkin Elmer. The Chl a and b content of solubilized thylakoids were measured after extraction in 80% acetone using extinction coefficients given by Arnon et al. 1949. The supercomplexes Low temperature (77° K) fluorescence emission spectra were registered by a FL55 spectrofluorometer (Perkin Elmer), equipped with a red sensitive photomultiplier and a low temperature cuvette holder. Samples were excited at 436 nm. The spectral bandwidth was 7.5 nm (excitation) and 5.5 nm (emission). The Chl concentration was approximately 0.5 mg ml in 90% (v/v) glycerol/sucrose gradient buffers.

2.6 Biochemical characterization of solubilized membranes and of isolated supercomplexes.

The protein composition of supernatants obtained after the solubilization treatments and the supercomplexes isolated by ultracentrifugation were investigated by native and non-denaturing analyses (BN-PAGE and size-exclusion chromatography) and by electrophoresis under denaturing conditions (SDS-PAGE). Protein complexes from solubilized thylakoids and the isolated PSII-LHCII supercomplexes were separated by BN-PAGE (Schagger and von Jagow, 1991) using a linear gradient gel (3–12% acrylamide). For molecular mass markers, a mixture of lyophilized standard proteins (Amersham, high molecular weight, GE Healthcare) was used. For the second dimension, the BN-PAGE lanes were cut out and denatured in a buffer made of 66 mM Na_2CO_3, 2% (w/v) SDS and 0.66%

(v/v) 2-mercaptoethanol at 25 °C for 30 min and subjected to SDS-PAGE on 15% polyacrylamide gel containing 6 M urea (Laemmli et al. 1970). The same electrophoretic system was used for mono-dimensional SDS-PAGE also for isolated PSII-LHCII supercomplexes with the only modification being the lowering of polyacrylamide to 12.5%. Pre-stained protein size markers (Bio-Rad, Precision Plus) were used for estimation of apparent size of components.

The separated proteins were visualized by Coomassie brilliant blue R-250 or silver staining. The same supernatants used for electrophoresis and the sucrose gradient bands corresponding to PSII-LHCII supercomplexes were subjected to size-exclusion chromatography on a Jasco HPLC system with a BioSep-SEC-S 3000 (Phenomenex) column. The 20 µl samples injected contained 6 µg Chl and the profiles were monitored at 400 nm. The mobile phase consisting of 20 mM MES pH 6.5, 10 mM $MgCl_2$, 30 mM $CaCl_2$, 0.5 M mannitol and 0.59 mM α-DM or β-DM passed through the column at a flow rate of 0.5 ml/min. To collect peaks of the thylakoid supernatants, the flow rate of the mobile phase through the column was reduced to 0.2 ml/min, and after the appearance of the first green material, fractions of 0.4 ml each were collected. Fractions containing peaks were kept on ice and analyzed within 1 h by absorption spectroscopy and loaded on SDS-PAGE.

PSII-LHCII supercomplexes were subjected also to SDS-PAGE Tris–Tricine system (Danielsson et al. 2006) with a 16% acrylamide resolving gel containing 6 M urea. Pre-stained protein size markers (Precision plus, Bio-Rad) were used for the estimation of apparent size of PSII–LHCII components. Moreover both PSII-LCII supercomplexes were subjected to mono-dimensional SDS-PAGE performed on a linear gradient gel (18-22% acrylamide) containing 6 M urea (Kashino et al. 2001) to improve the resolution of LMM subunits. The separated proteins were either stained by Coomassie brilliant blue R-250 or transferred onto nitro-cellulose membrane and immuno-detected with specific antisera against LHCII subunits and PsbO, PsbP, PsbR, PsbW and PsbS polypeptides, by using the alkaline phosphatase conjugate method, with 5-bromo-4- chloro-3-indolyl phosphate/nitro blue tetrazolium as chromogenic substrates (Sigma).

2.7 Mass spectrometry

For liquid nano chromatography electrospray ionization tandem mass spectrometry (nanoLC-ESI-MS/MS) analysis, spots from the 2D SDS-PAGE and bands from the 1D SDS-PAGE were cut out and proteins were digested in-gel with trypsin (Roche) as in Hellmann et al. 1995. NanoLC-ESI-MS/MS

data from each protein sample were obtained by using a Q-star XL (AB SCIEX) as in Pagliano et al. 2011. Mascot.dll v 1.4804.0.22 (Matrix Science/AB SCIEX) was used to generate Mascot (.mgf) files with peak lists from the Analyst QS 2.0 (.wiff) files. The MS/MS spectra, that were obtained using digested samples, were analyzed as Mascot generic files against all entries in the public NCBInr database using the online Mascot server (Matrix Science: http://www.matrixscience.com/) without a taxonomy filter.

The principal parameter settings for the Mascot search were as follows: database NCBInr (version 2012.02.26; containing 17406376 sequence entries); enzyme trypsin; allow up to one missed cleavage; possible variable modifications carbamidomethylation of cysteine (C), oxidation of methionine (M), deamidation of asparagine and glutamine (NQ); precursor ion mass and fragment masses tolerance respectively of 60 ppm and 0.3 Da; instrument ESI-QUAD-TOF; default charge state set to 2+, 3+, and 4+. Widely accepted procedures for positive identifications of proteins by MS/MS analysis require a minimum of two unique peptides with at least one peptide having a significant ion score (p=0.05). Considering that the genome of *Pisum sativum* is not fully sequenced, and that only some protein sequences of *Pisum sativum* are present in the database, we also accepted, as confident assignments, hits identified by at least one peptide with a significant ion score according to the MASCOT MS/MS ion search algorithm. For matrix-assisted laser desorption/ionization-time of flight (MALDI-TOF) and matrix-assisted laser desorption/ionization-time of flight/time of flight (MALDI-TOF/TOF) MS analyses, the isolated PSII-LHCII supercomplexes were initially dialyzed for 18 h against 5% (v/v) acetic acid, using a 12-14 kDa cut-off membrane (Spectra/Por, SpectrumLabs), and further concentrated to 1/10 of the initial volume by membrane filtration with Amicon Ultra 100 kDa cut-off devices (Millipore). 1 µl of each concentrated sample was mixed with 9 µl of saturated matrix (sinapic acid, Laser Biolabs) solution which consists of 60% (v/v) acetonitrile and 0.1% (v/v) trifluoroacetic acid. After drying droplets of sample onto a target plate, MALDI-TOF and MALDI-TOF/TOF MS analyses were performed using respectively the mass spectrometers Voyager-DE PRO MALDI-TOF (AB SCIEX) and MALDI-TOF/TOF TM 800 System (AB SCIEX).

The MALDI-TOF mass spectrometer was operated in linear mode at 25 keV accelerating voltage, grid 96.5%, guide wire 0.05% and 800 ns ion extraction delay; the nitrogen laser working at 337 nm and 3 Hz. Two hundred laser shots were accumulated per spectrum over a *m/z* range of 3,500–10,000. Internal calibration was performed on the samples premixed with Calibration mixture 2 of the Peptide Mass Standards Kit for Calibration of AB SCIEX MALDI-TOF Instruments. MALDI TOF-TOF spectra were acquired using the AB SCIEX TOF/TOF TM 5800 system operated with positive

ionization either in linear mode, to determine the average molecular mass, or in reflector mode, to analyze the fragments. An internal calibration was performed on the samples premixed with polyethylene glycol (PEG4000). MS/MS was carried out on the top precursors. Between twenty thousand and two hundred thousand shots were accumulated to get the best S/N, with laser frequency of 1 kHz, acceleration voltage of 2 keV and using air as collision gas. The MS/MS spectra, obtained from the main proteins peaks in MS, were analyzed in Mascot Distiller (ver. 2.3.2.0) by the *de novo* sequencing function coupled with MS-Blast (http://dove.embl.de/Blast2/msblast.html) search at EMBL http://www.embl.de/ using default parameter values.

2.8 Oxygen evolution measurements

The oxygen evolution was measured at 20° C using a Clark-type oxygen electrode (Hansatech) under saturating light intensity (~1000 and 5000 µmol m^{-2} s^{-1} photons, respectively, for thylakoids and PSII-LHCII particles). Chl of thylakoids (10 µg) and 25 or 20 µg Chl of PSII-LHCII particles isolated, respectively, with α-DM or β-DM were added to 1 ml of a medium made of 25 mM MES pH 6.5, 2 M glycine betaine, 10 mM $NaHCO_3$, 10 mM NaCl, in the presence or absence of 25 mM $CaCl_2$. A mixture of 1 mM $K_3Fe(CN)_6$ and 200 mM DCBQ or 500 mM DCBQ alone were used as electron acceptors for thylakoids and PSII–LHCII particles, respectively.

2.9 Transmission electron microscopy 2D and 3D single particle image analysis

Samples from sucrose gradient bands were diluted 10-fold in a buffer composed of 10 mM HEPES pH 7.5 and stained with 2 % uranyl acetate on glow discharged carbon-coated copper grids. EM was performed with a Phillips CM200FEG electron microscope operated at 200 kV. The images were recorded at 50 000 on a TVIPS F415 4Kx4K CCD camera leading to a final pixel size of 1.76 Å at specimen level. A dataset of 15,563 negatively stained single particle images were obtained by picking all discernible single particles present. Several sub-populations of particles, differing in size and shape, were identified. The two largest sub-populations, corresponding to the $C_2S_2M_2$ and the C_2S_2 PSII-LHCII supercomplexes, were in turn analysed as separate datasets, with the reference free alignment giving the initial class averages necessary for multi-reference alignment. Single particle analysis was performed using EMAN2 (Tang et al. 2006) and IMAGIC softwares, including initial reference-free alignment, followed by multireference alignment and multivariate statistical analysis and classification. (van Heel et al. 2011).

The modelling studies of the two-dimensional projection maps were conducted with X-ray structures of the PSII core of cyanobacteria at 1.9Å (Umena et al. 2011) the LHCII complex of pea at 2.5 Å (Standfuss et al. 2005) and the CP29 of spinach at 2.8 Å (Pan et al. 2011) using UCSF Chimera (Pettersen et al. 2004).

Relative orientations were determined for the class averages by the angular reconstitution technique (van Heel, 1987) and initial 3D reconstructions gained from implementation of the exact back projection technique (Radermacher, 1988). Reprojections were taken from each 3D model and used to identify additional atypical views and further refine the class averages within each sub- population dataset. Through iterative refinement the data converged to give the best 3D reconstructions shown. Resolution was determined by calculating the Fourier shell correlation (FSC) at the 3scriterion between two independent 3D reconstructions (van Heel and Schatz, 2005). Relevant crystallographic co-ordinate atom data were modelled into molecular maps derived from the sub-populations using PyMOL (The PyMOL Molecular Graphics System, Version 1.1r1, Schrödinger, LLC) and UCSF Chimera modelling software. Surface rendered views were calculated at a threshold of 2.5 s.

RESULTS

3. RESULTS

3.1 Comparison of the α and β isomeric forms of the detergent n dodecyl-D-maltoside for solubilizing photosynthetic complexes from pea thylakoid membranes.

3.1.1 Aim of the work

In order to compare the two isomeric forms of DM, identify the optimal concentrations and to isolate PSII-LHCII supercomplexes, we have carried out an analysis of the action of the α- and β-DM on thylakoid membranes of the higher plant *Pisum sativum*. The supernatants obtained by solubilization have been analyzed with biochemical techniques as: spectrophotometric analysis, BN-PAGE to preserve their native organization and denaturing SDS-PAGE to determine their polypeptide compositions.

3.1.2 Overview of the results

First of all, it has been carried out the solubilization at 1 mg/ml of *Pisum sativum* stacked thylakoid with increasing concentrations of both detergents from 5 mM to 100 mM. The obtained supernatants have been analyzed with spectrophotometric techniques.

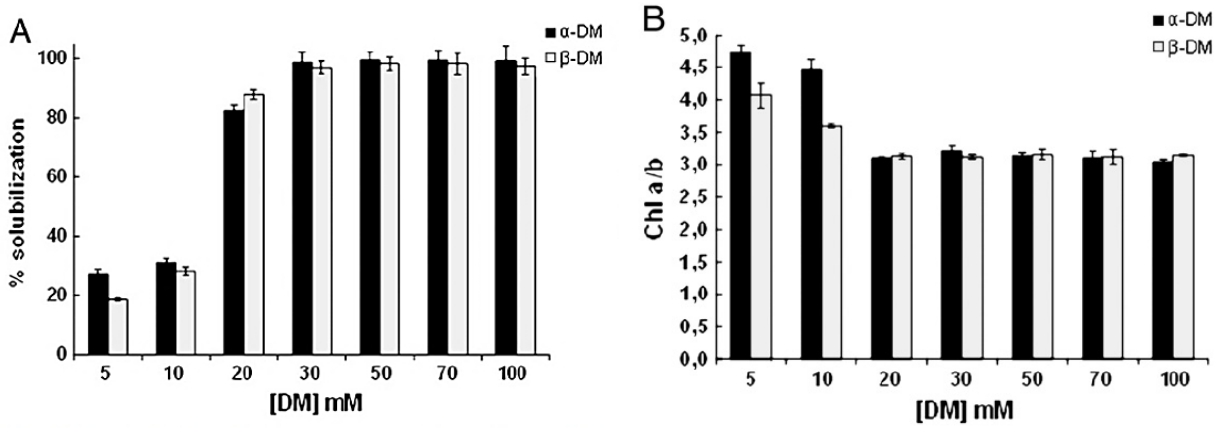

Figure 3.1.1. A. Degree of thylakoids solubilization with increasing concentrations of α-DM and β-DM. B. Chl a/b ratios of thylakoids solubilized with different concentrations of α-DM and β-DM, where Chl a/b ratio of starting thylakoids is 3.15 ± 0.03. Chlorophyll concentrations and Chl a/b ratios were determined in 80% acetone using the extinction coefficients reported by D. J. Arnon, 1949. Each value is the average of at least ten independent determinations.

The data obtained by spectrophotometric analysis show that the complete solubilization is achived, for both detergents, from 30 to 100 mM (figure 3.1.1, A) and the Chl *a/b* ratios values of each supernatants are the highest at low concentrations of both detergents (figure 3.1.1 B). The supernatants have been loaded on to BN-PAGE in order to separate the membrane complexes in their native form. In both BN-PAGE (figure 3.1.2. A and B), from 5 to 20 mM, it is clearly visible that some solubilized materials haven't been entered in the resolving gel, in correspondence of the wells.

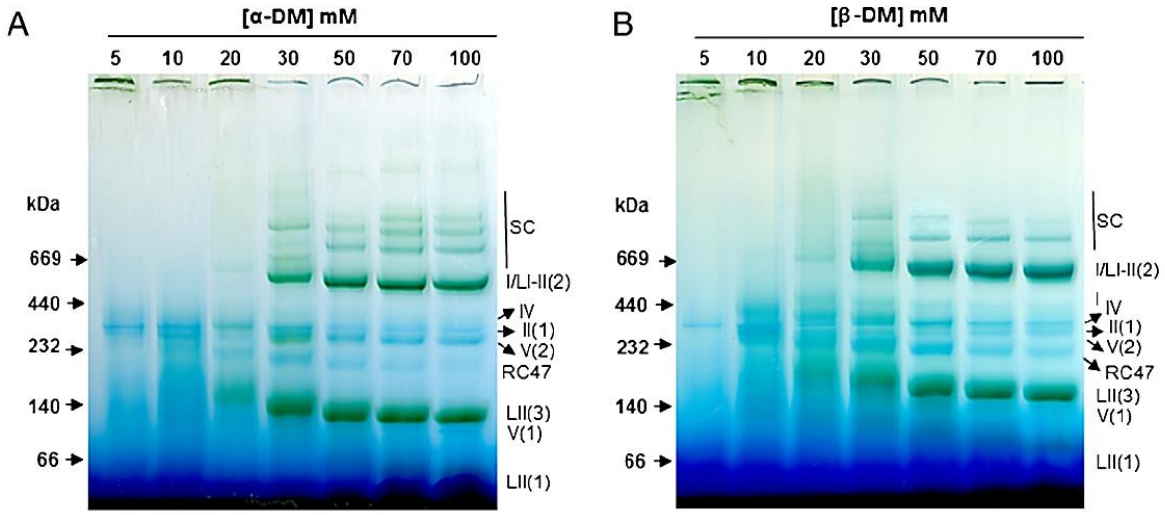

Figure 3.1.2. A–B. BN-PAGEs of pea thylakoids solubilized with increasing concentrations of α-DM (A) and β-DM (B). Lane 1, native high molecular weight marker (GE Healthcare); lanes 2–8, pea thylakoids (20 µg Chl) solubilized with increasing concentrations of detergent. Isolated complexes and subcomplexes were indexed as follows: supercomplexes (SC), PSI (I), PSII (II), LHCI (LI), LHCII (LII), ATP-ase (IV), Cyt b_6f complex (V). Arabic numbers were added in brackets to indicate the oligomeric status of the protein complex as, trimeric (3), dimeric (2) and monomeric (1).

It is likely that the thylakoids at these concentrations haven't been fully solubilized. From 30 to 100 mM, both detergents instead, are able to solubilized all the protein complexes embedded in the thylakod membranes. In particular from 50 mM to 100 Mm in gel A are visible three bands and in gel B two bands above 669 kDa. In order to determine the polypeptide composition of each separated complexes we have cut the lanes corresponding to 70 mM of both gels and loaded them on 2D (Figure 3.1.3).

So they have been identified three different PSII-LHCII supercomplexes for A gel and two for B gel; ATP- ase, PSII dimer, and PSI-LHCI ; Cyt b_6f complex and PSII monomer; LHCII trimers and LHCII monomers.

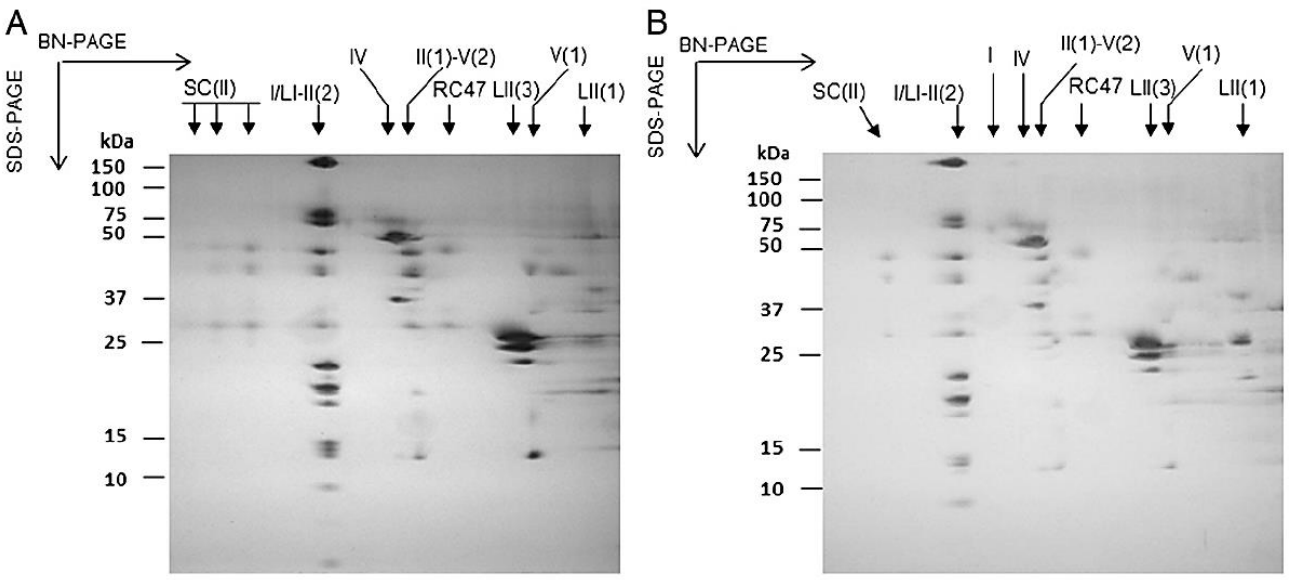

Figure 3.1.3. Second dimension SDS-PAGEs. The BN-PAGEs of stacked thylakoids solubilized with 70 mM α-DM (A) and 70 mM β-DM (B) were subjected to SDS-PAGE. The second dimensions were silver stained. Labels on the left of the SDS-PAGEs indicate the molecular weight positions, symbols above indicate the correspondence between thylakoids protein complexes (indexed as in 3.1.2) in the first dimension and their polypeptide composition in the second dimension.

3.2 Characterization of PSII-LHCII supercomplexes isolated from pea thylakoid membranes by one-step treatment with α- and β-dodecyl-D-maltoside.

3.2.1 Aim of the work:

In this second work, taking into account the preavious thylakoid membranes solublization results, they have been characterized two forms of PSII-LHCII supercomplexes isolated with 50 mM α and β-n-dodecil maltoside from the same thylakoid membanes. In the first step they have been characterized them by using biochemical techniques such as spectrophotometric analysis, SDS-PAGE, immuno blotting, HPLC-size exclusion and 77 K fluorescence. Moreover they have been carried out oxygen evolution measurements in order to verify the functionality of both isolated supercomplexes. In the second step they have been obtained 2D projection maps by using EM single particle analysis of both supercomplexes.

3.2.2 Overview of the results:

First of all, they have been fractionated the solubilized thylakoids at 50mM of both detergents on linear sucrose gradient. In figures 3.2.1 are represented alfa and beta gradients. Both gradients presents three intense bands in the same position and two faint bands differently localized. Thye have been named and collected each bands for the biochemical characterization.

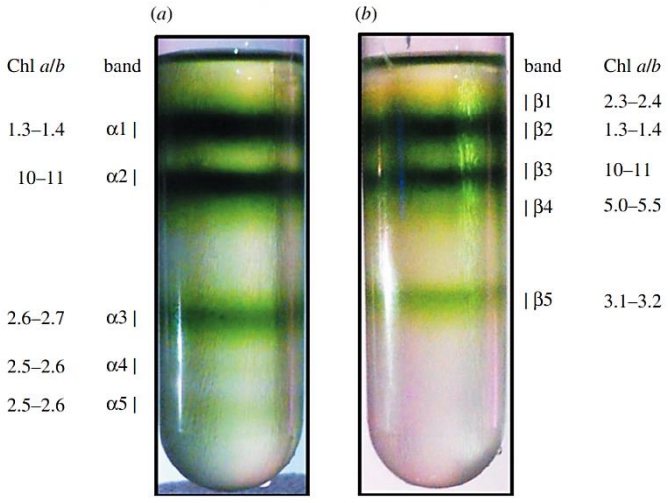

Figure 3.2.1. Separation of pigment-binding complexes by sucrose gradient ultracentrifugation of thylakoids solubilized with (a) α-DM and (b) β-DM

Each collected bands were loaded on to SDS-PAGE in order to determine their polypeptide composition (figure 3.2.2.).

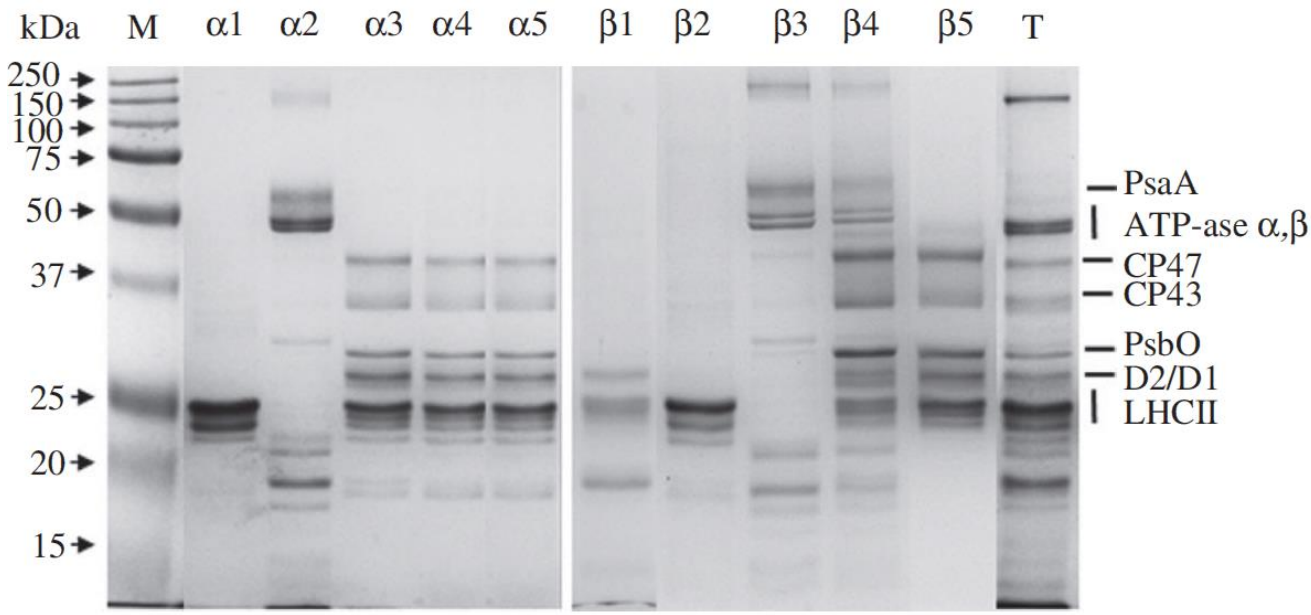

Figure 3.2.2. Protein composition of sucrose gradient bands a1–a5 isolated from thylakoids solubilized with α-DM, of bands b1–b5 isolated from thylakoids solubilized with β-DM and of thylakoid membranes (lane T). Chl (4 mg) was loaded on each lane. On the left-hand side, pre-stained protein markers with indicated apparent molecular weight (kDa).

The gels represented in figure 3.2.2 show that in the alfa gradient they have been separated from the top of the tube: LHCII trimers (lane α1), PSI plus ATP-ase α and β subunit (lane α2), and three PSII-LHCII supercomplexes (lane α3, 4 and 5). In the beta gradient, instead, they have been separated: LHCII monomers (lane β1), LHCII trimers (lane β2), PSI plus ATP-ase a and b subunit (lane β3), a mixture of PSI plus ATP-ase α and β subunit and PSII core subunits (lane β4) and PSII-LHCII supercomplex (lane β5).We have focused our attention on the intense green bands named α3 and β5 contains PSII-LHCII supercomplexes hereafter that will be call them α-supercomplex and β–supercomplex.

They have been subjected α-supercomplex and β–supercomplex to tricine SDS-PAGE (according to Schagger and von Jagow, 1991) and immunoblotting.

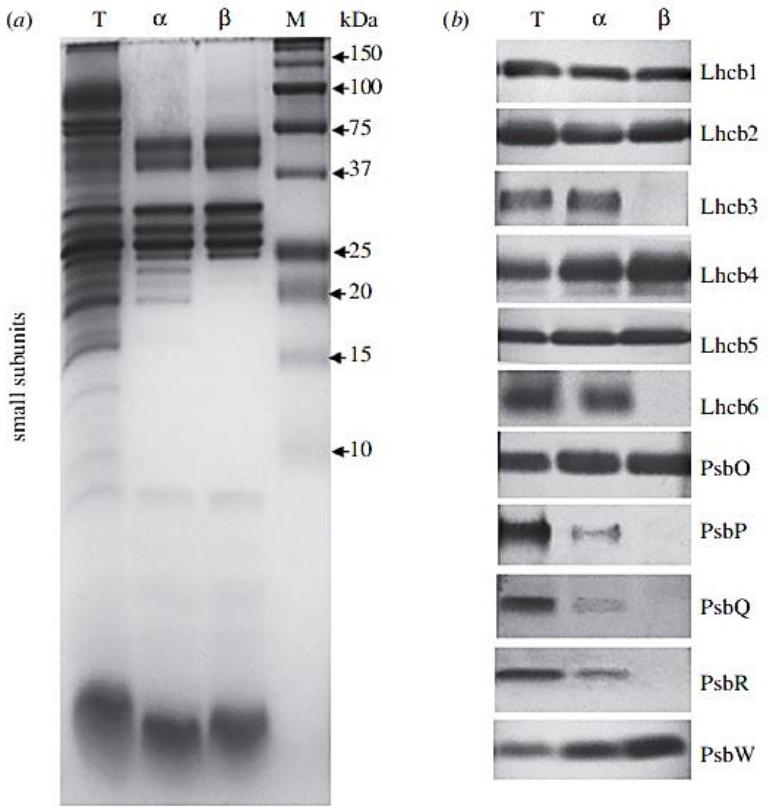

Figure 3.2.3. Protein composition of α-supercomplex (a) and β-supercomplex (b) and of pea thylakoids (lane T). Chl (8 mg) was loaded on each lane. Lane M, pre-stained protein markers with their apparent molecular weight (kDa) indicated. (b) Western blot with antibodies against antenna polypeptides Lhcb1-6, OEC subunits PsbO, PsbP, PsbQ and PsbR and PsbW of α-supercomplex (a) and β-supercomplex (b) and of pea thylakoids (lane T). Chl (1 mg) was loaded on each lane.

The tricine gel show that α-supercomplex contains more subunits than β–supercomplex (figure 3.2.3 panel (a)). With immunoblotting they have been identified these subunits, in fact, unlike the β–supercomplex, the α-supercomplex contains also Lhcb3 and Lhcb6, PsbP, PsbQ and PsbR (figure 3.2.3 panel (b)). It seems that the α-supercomplex is the most intact. In order to understand better how these supercomplexes are made, in particular their differences in antennae size, we have carried out the structural analys by using EM negative stain and single particle analisys method.
The bands corresponding to α-supercomplex and β-supercomplex were deconcentrated and negative stained with uranyl acetate and observed with TEM. They have been taken more than 600 micrographs for both supercomplexes. We have focused our attention on the ~6000 top-views for α-supercomplex and ~7000 for the β–supercomplex. The two datasets obtained were separately processed. The final results have shown that the collected particles in the α-supercomplex sample were $C_2S_2M_2$

supercomplexes, and in β-supercomplex sample were of C_2S_2 supercomplexes. The homogenous top-views projection of both supercomplexes have been summed in order to obtain the final projection maps represented in figure 3.2.4.

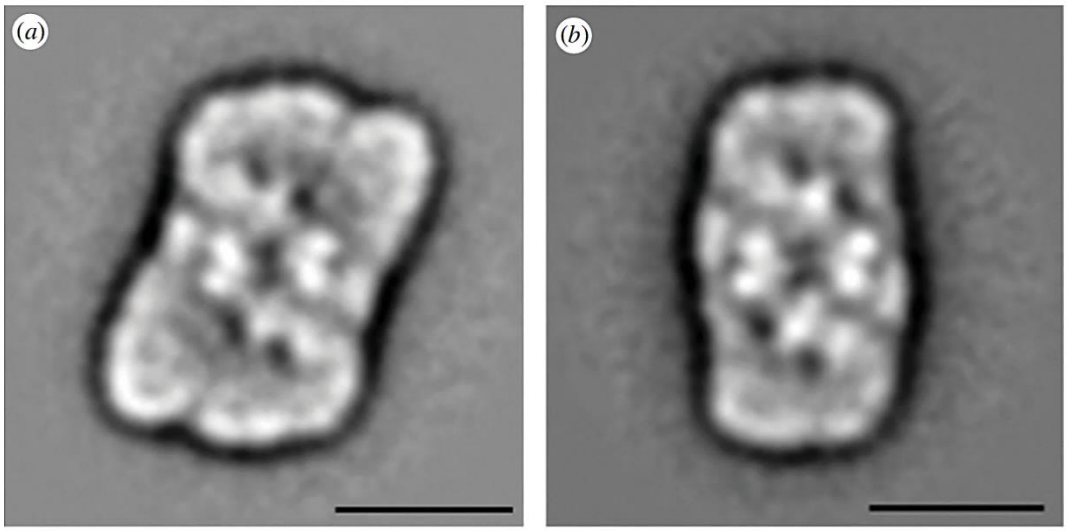

Figure 3.2.4. Final projection maps of the $C_2S_2M_2$ supercomplex isolated with α-DM and (b) the C_2S_2 supercomplex isolated with β-DM. The scale bar equals 150 A.

In order to assign the name of all the subunits they have been superimposed on the final projection maps of the $C_2S_2M_2$ and the C_2S_2 (in figure3.2.5 panel c and in panel d respectively) the high resolution structures of the PSII core and the LHCII proteins.

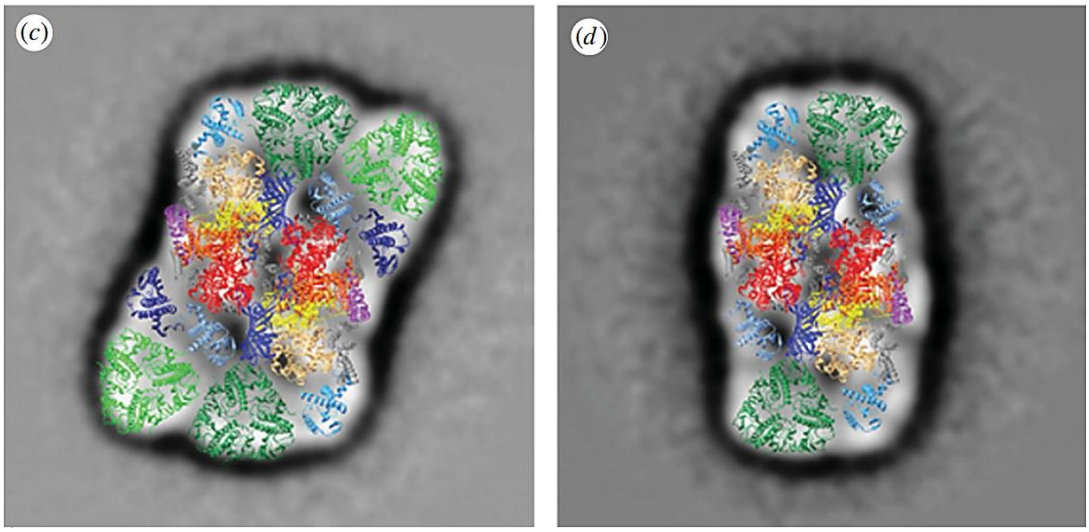

Figure 3.2.5. Assignment of the subunits in the $C_2S_2M_2$ and (d) C_2S_2 supercomplexes by fitting the high-resolution structures of the PSII core (Umena et al. 2011) (subunits D1, D2, CP47, CP43 and PsbO are in yellow, orange, red, sandy brown and blue, respectively), the LHCII (Standfuss et al. 2005) (S-trimer is in dark green and M-trimer in light green) and the monomeric Lhcb (Pan et al. 2011) (CP29, CP26 and CP24 are in steel blue, turquoise and dark blue, respectively).

3.3 Proteomic characterization and three dimensional electron microscopy study of PSII-LHCII supercomplexes from higher plants.

3.3.1 Aim of the work:

In this third work we analyzed the protein composition, by applying mass spectrometry, of C_2S_2 and $C_2S_2M_2$ supercomplexes isolated preaviously. In this way, we have revealed the presence of the antenna proteins Lhcb3 and Lhcb6 and of the extrinsic polypeptides PsbP, PsbQ and PsbR exclusively in the $C_2S_2M_2$ supercomplex. Other proteins of the PSII core complex, common to the $C_2S_2M_2$ and C_2S_2 supercomplexes, including the low molecular mass subunits, were also detected and characterized. To complement the proteomic study with structural information, we performed negative stain transmission electron microscopy and single particle analysis to calculated 3D electron density maps for the $C_2S_2M_2$ and C_2S_2 supercomplexes, approaching respectively 30 and 28 Å resolution.

3.3.2 Overview of the results:

We have subjected both supercomplexes, isolated as in Barera et al. 2012, to further electrophoretic analysis such as BN-PAGE and the 2D SDS-PAGE in order to obtain informations about the size and the polypeptidic composition of both supercomplexes. The BN-PAGE confirmed the $C_2S_2M_2$ has a higher molecular mass than C_2S_2 and pointed out that some of the $C_2S_2M_2$ population loss LHCII trimers (visble in the bottom of the gel in figure 3.3.1 A). Consequently, below the band of $C_2S_2M_2$ is present a faint band of small supercomplex with molecular mass similar to the C_2S_2. It is likely that the LHCII trimer in the bottom of the gel is a proportion of M trimers lost by $C_2S_2M_2$ supercomplex during the electrophoretic run. We have carried out the also the 2D SDS-PAGE with loaded both the lanes of the BN-PAGE (figure 3.3.1 B).

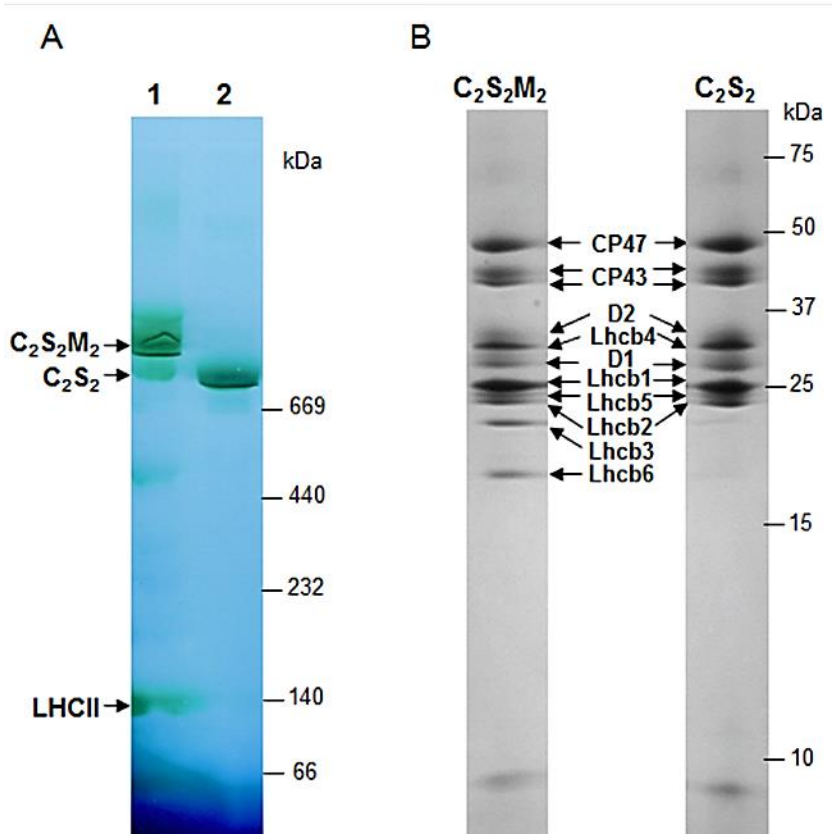

Figure 3.3.1. BN/2D SDS-PAGE profiles of PSII-LHCII supercomplexes isolated from pea thylakoid membranes. A. BN-PAGE of $C_2S_2M_2$ supercomplex (lane 1) and C_2S_2 supercomplex lane 2) (6 µg Chl per lane). Protein marker (Native high molecular mass, GE Healthcare) positions indicated on the right. B. 2D SDS-PAGE separation of $C_2S_2M_2$ and C_2S_2 supercomplexes, after Coomassie staining. Protein marker (Precision plus, Bio-Rad) positions indicated on the right.

In order to analyze the LMM component and obtain a better resolution of all subunits of both supercomplexes we have carried out another high resolution gel according to Kashino et al. 2001 method. (figure 3.3.2).

We have cut and digested with trypsin the $C_2S_2M_2$ spots from the 2D SDS-PAGE and from the Kashino gel and carried out LC ESI MS/MS spectrometry.

We have identified with high score in $C_2S_2M_2$: CP47, CP43, D1, D2, all the Lhcb proteins, the OEC proteins PsbO, PsbP and PsbQ, the protein PsbR and only 2 low molecular masses ubunits PsbE and PsbH. The mass spectrometry results have been reported in table 3.1.

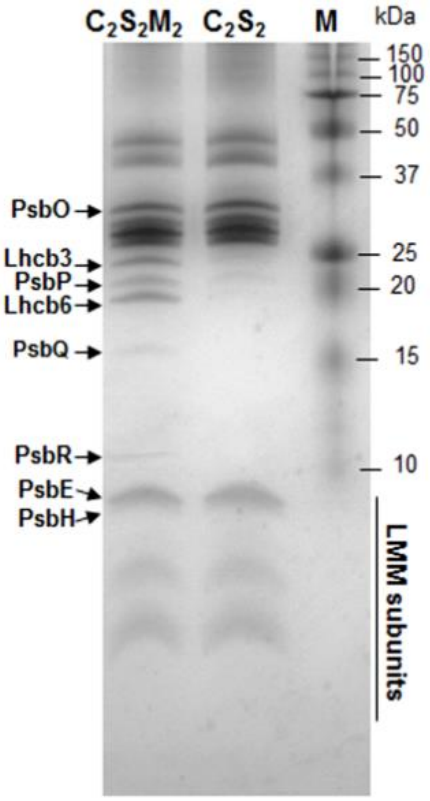

Figure 3.3.2 Profiles of protein composition of $C_2S_2M_2$ and C_2S_2 supercomplexes (10 µg Chl per lane) resolved by 1D SDS-PAGE according to (Kahino et al. 2001). Protein standards (Precision plus, Bio-Rad) are loaded on lane M.

Protein	Precursor ion mass *m/z*	Sequence	Mr (kDa)	AC number (gi NCBI) reference organism	% Identity with *P. sativum or A. thaliana* (sequence coverage)
CP47	1922.8587 1759.8741 1484.7299 2186.0215 1289.6615	YQWDQGYFQQEIYR VGGGLVENQSLSEAWSK LAFYDYIGNNPAK AGSMDNGDGIAVGWLGHPIFR AQLGEIFELDR	54208	gi|27446507 (*Pisum sativum*)	100% gi|27446507 *P. sativum* (15%)
CP43	1708.7594 1890.9952 1818.8822	DQETTGFAWWAGNAR APWLEPLRGPNGLDLSR GIDRDFEPVLSMTPLN	51955	gi|295136994 (*Pisum sativum*)	100% gi|295136994 *P. sativum* (10%)
D2	2044.9160 1226.5931 1546.6827 1040.5978 2636.2693	AFNPTQAEETYSMVTANR AYDFVSQEIR AAEDPEFETFYTK NILLNEGIR AWMATQDQPHENLIFPEEVLPR	35386	gi|27435890 (*Pisum sativum*)	100% gi|27435890 *P. sativum* (10%)
D1	1458.7255 1313.7092 1110.5458	LIFQYASFNNSR VINTWADIINR NAHNFPLDLA	38962	gi|131252 (*Pisum sativum*)	100% gi|131252 *P. sativum* (9%)
PsbO	1235.6510 2440.1329 1421.7588 2269.1002 2293.1226 963.5793 2283.1535 2433.1408 3359.7348 1292.6401	RLTFDEIQSK GTGTANQCPTIDGGVDSFSFKPGK KLCLEPTSFTVK LTYTLDEIEGPFEVSADGSVK FEEKDGIDYAAVTVQLPGGER VPFLFTIK QLVASGKPDSFSGEFLVPSYR GASTGYDNAVALPAGGRGDEEELGK ITLSVTQTKPETGEVIGVFESIQPSDTDLGAK IQGVWYAQLES	34872	gi|131384 (*Pisum sativum*)	100% gi|131384 *P. sativum* (59%)
PsbP	1604.6995 2373.1336 1571.7355 3396.6474 1255.6561 1839.9327 1386.6667	TNTDYLPYNGDGFK YEDNFDATSNVSVLVQTTDKK SITDYGSPEEFLSK QAFFGQTDSEGGFDTNAVAVANILESSAPVIGGK QYYNISVLTR TADGDEGGKHQLITATVK KFVEDTASSFSVA	28030	gi|131390 (*Pisum sativum*)	100% gi|131390 *P. sativum* (48%)

PsbQ	1990.0120 1110.6761 1655.8770 1258.6458 1470.7467 1530.8194	VGGPPPLSGGLPGTLNSDEAR DLKLPLKER FFIQPLAPTEAAAR AWPFLQNDLR LFQDISNLDHAAK YYAIAVSTLNDVLSK	25265	gi|31096349 (*Pisum sativum*)	100% gi|31096349 *P. sativum* (35%)
PsbR	2537.2068 2608.2486	IKTDTPYGTGGGMDLPNGLDASGRK GVYQFVDKYGANVDGYSPIYEPK	14170	gi|33694227 (*Trifolium pratense*)	71% gi|15219268 *A. thaliana* (29%)
PsbE	1121.6081 953.5658 1484.6783	SFADIITSIR QGIPLITGR FDSLEQLDEFSR	9381	gi|293338576 (*Pisum sativum*)	100% gi|293338576 *P. sativum* (41%)
PsbH	1732.9247	TVVGDLLKPLNSEYGK	7824	gi|295137033 (*Pisum sativum*)	100% gi|295137033 *P. sativum* (23%)
Lhcb1	1377.6313 3944.7581 1251.6683 1934.9747 982.4913 4548.2999 3525.7555 3123.5050	VASSGSPWYGPDRVK YLGPFSGESPSYLTGEFPGDYGWDTAGLSADPETFSK NRELEVIHSR WAMLGALGCVFPELLSR FGEAVWFK AGSQIFSEGGLDYLGNPSLVHAQSILAIWATQVILMGAVEGYR IAGGPLGEVVDPLYPGGSFDPLGLADDPEAFAELK GPLENLADHLADPVNNNAWSYATNFVPGK	28635	gi|115788 (*Pisum sativum*)	100% gi|115788 *P. sativum* (72%)
Lhcb2	1601.7838 4053.8585 1950.9583 982.4913 3455.6773	SAPESIWYGPDRPK YLGPFSEQIPSYLTGEFPGDYGWDTAGLSADPETFAR WAMLGALGCTFPELLEK FGEAVWFK VGGGPLGEGLDPLYPGGAFDPLGLADDPDSFAELK	28866	gi|115797 (*Pisum sativum*)	100% gi|115797 *P. sativum* (43%)
Lhcb3	1247.6299 3926.7839 1901.9743 1293.6758	DLWYGPDRVK YLGPFSAQTPSYLTGEFPGDYGWDTAGLSADPEAFAK WAMLGALGCITPEVLQK VDFKEPVWFK	28710	gi|20671 (*Pisum sativum*)	100% gi|20671 *P. sativum* (24%)
Lhcb4	1768.8784 1315.6455 1418.7082 985.5808	STPFQPYTEVFGLQR FRECELIHGR FFDPLGLAADPEK ATLQLAEIK	31290	gi|346987811 (*Dimocarpus longan*)	80% gi|38502901 *A. thaliana* (16%)
Lhcb5	1157.6445 1497.6711	IFLPDGLLDR YGANCGPEAVWFK	30138	gi|15235029 (*Arabidopsis thaliana*)	100% gi|15235029 *A. thaliana* (8%)
Lhcb6	1854.8384	TAENFNNSTGLQGYPGGK	23518	gi|168009690 (*Physcomitrella patens*)	82% gi|4741960 *A. thaliana* (7%)

Table 3.1. List of PSII RC core subunits, extrinsic polypeptides, LMM subunits and LHCII proteins identified by nanoLC- ESI-MS/MS present in the isolated $C_2S_2M_2$ and C_2S_2 PSII-LHCII supercomplexes. The table reports: sequences of peptides obtained by nanoLC-ESI-MS/MS (third column) with their corresponding precursor ion mass (second column); for each identified protein (first column), the calculated molecular mass (Mr, fourth column), the accession number and the database in which the protein was found (fifth column), and the percentage of residue identities with *Pisum sativum,* when available, or the homolog *Arabidopsis thaliana* (sixth column). Underlined amino acid residues (third column) indicate modifications such as carbamidomethylation of cysteine (C), oxidation of methionine (M), deamidation of asparagine and glutamine (N, Q).

We have carried out also MALDI/TOF and TOF/TOF analysis in order to obtain further informations about the LMM component. In figure 3.3.3 are represented the MALDI/TOF spectra of both Supercomplex. Both spectra have the same profile and we identify four subunits (in orange) by using a putative assignment from data present in literature. The other proteins, in blue, have been identified by using de novo sequencing assignment with MALDI TOF/TOF analysis.

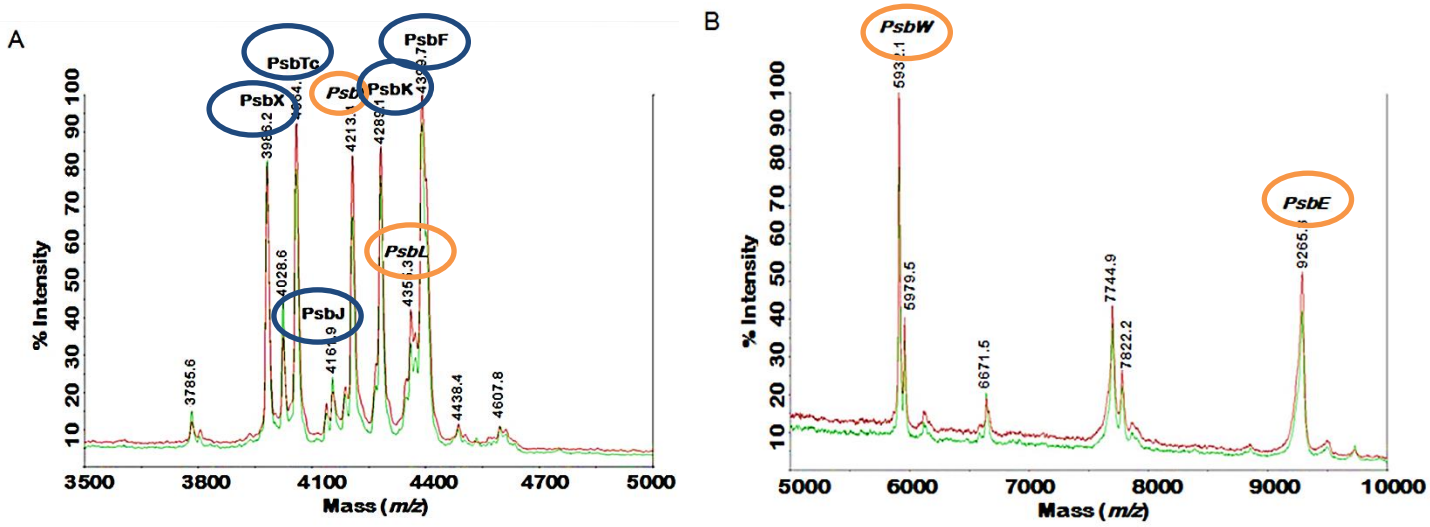

Figure 3.3.3. MALDI-TOF mass spectra of PSII-LHCII supercomplexes of type $C_2S_2M_2$ (green line) and C_2S_2 (red line) isolated from pea thylakoid membranes. A. Peaks with m/z values between 3,500-5,000. B. Peaks with m/z values between 5,000-10,000.

In addition to the proteomic characterization of both supercomplexes we have carried out negative stain transmission electron microscopy and single particle analysis to calculated 3D electron density maps for the $C_2S_2M_2$ and C_2S_2 supercomplexes. In the current study, the preavious dataset (Barera et al. 2012) was re-subjected to more intensive computer-based purification analyses, so that more rigorously defined sub-populations of particles might be identified prior to the application of the 3D reconstruction technique of angular reconstitution. In so doing, sub-populations of 4,760 and 1,868 particles were identified relating to the largest complexes, in terms of surface area with two-fold symmetry.

Following *de novo* reference-free alignments, the relative angular orientations of the particles observed within each sub-population were strongly biased towards top and side views; however, subsequent iterative refinements were able to identify a small amount of slightly tilted views which aided in the calculation of the final 3D electron density maps.

The $C_2S_2M_2$ map has maximum dimensions of 375 Å length by 210 Å width by 105 Å height and an approximate resolution of 30 Å. The C_2S_2 map is also shown with two-fold imposed symmetry, having dimensions of 340 Å length by 200 Å width by 105 Å height with a resolution of ~28 Å.

To interpret these 3D electron density maps, we compared their internal density distribution with surface-rendered X-ray structures (Figure 3.3.4 B C and D) of the PSII dimeric core of cyanobacteria at 1.9 Å (Umena et al. 2011) the LHCII trimeric complex of pea at 2.5 Å (Standfuss et al. 2005) and the monomeric Lhcb4 of spinach at 2.8 Å (Pan et al. 2011).

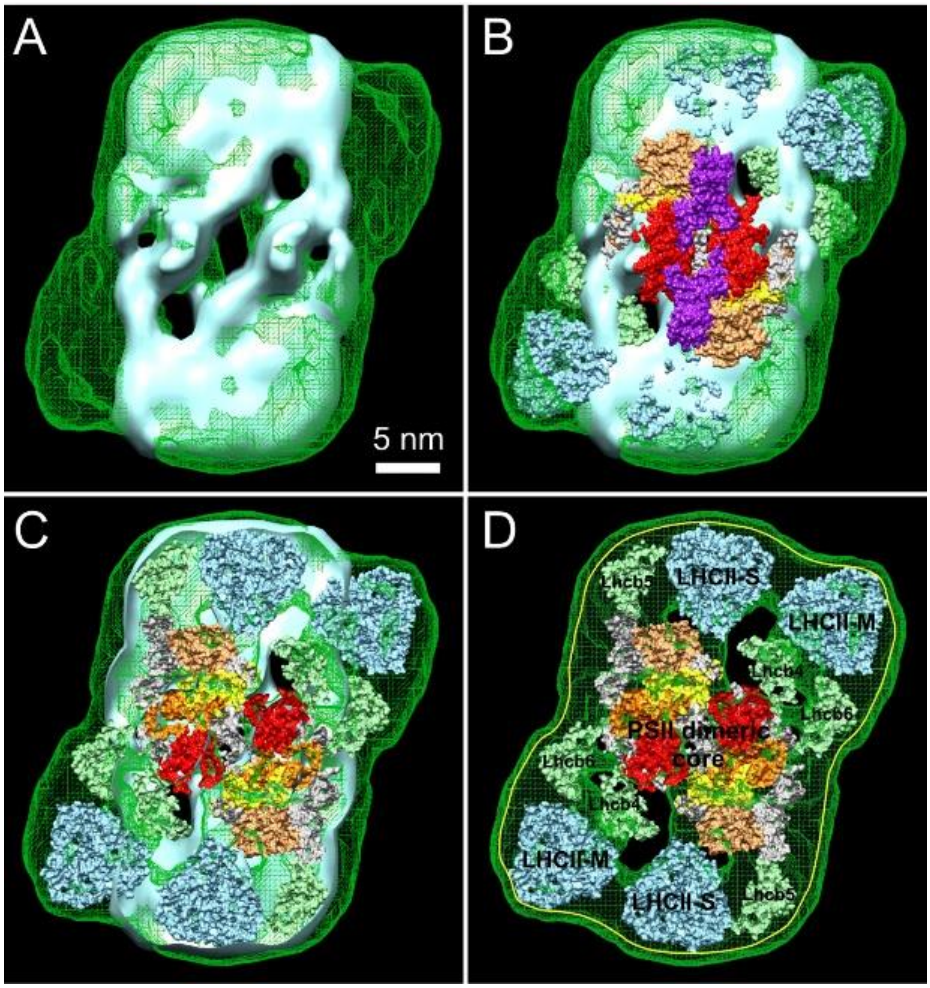

Figure 3.3.4 Top lumenal views of 3D reconstructions of the $C_2S_2M_2$and C_2S_2 supercomplexes, with modelled high-resolution X-ray structures of the PSII dimeric core from cyanobacteria (subunits D1, D2, CP47, CP43 and PsbO are in yellow, orange, red, sandy brown and purple, other subunits in grey, respectively), the LHCII trimer (in blue) and Lhcb4 (in pale green) A. Top lumenal view of the $C_2S_2M_2$ 3D electron density map (green mesh), with the C_2S_2 3D electron density map, inset, surface-rendered in light blue. B. As per panel A, highlighting lumenal surface differences, together with LHCII trimer and monomeric Lhcb atomic co-ordinates shown as surface- rendered spheres (coloured as described above). C. The modelling environment, cut away by 65 Å, to reveal its lower half, also 65 Å thick, thus emphasising the position of the X-ray co-ordinates (surface-rendered and coloured as described above). D. The $C_2S_2M_2$ 3D cut away map (as in C) on its own with modelled subunits labelled (surface-rendered and coloured as described above), its membrane domain also shown as a 65 Å thick slab from the lumenal top view. The Lhcb5 and Lhcb6 atomic co-ordinates, whose structures have not yet been solved, are assumed to be similar to that of Lhcb4. A delineating boundary (yellow line) represents the α-DM detergent shell, approximately 10 Å within the outer edge of the C_2S_2M three-dimensional mesh.

GENERAL DISCUSSION

4. GENERAL DISCUSSION

4.1 Comparison of the α and β isomeric forms of the detergent n-dodecyl-D-maltoside for solubilizing photosynthetic complexes from pea thylakoid membranes.

In this first work we have compared the action of the two isomeric forms of n-dodecyl-D-maltoside α and β by solubilizing at increasing concentrations identical stacked thylakoids (same lipid/Chl and protein/Chl ratios) with the aim to establish the best conditions to isolate fully solubilized PSII-LHCII supercomplexes and the other protein complexes in their native form. The differences obtained from thylakoid solubilization with either isomers, are discussed taking in to account the amount of detergent used in relationship with the different distribution of the protein complexes in the thylakoid membranes.

At 5 and 10 mM of both DM isomers we have obtained only a partial solubilization of thylakoids (30% of the initial membranes). The supernatant mainly consist of: small membrane fragments (the material that did'nt enter in the BN-PAGE represented in figure 3.1.2 A and B). The 5 and 10 mM supernatants Chl a/b ratio is higher than the other supernatants, suggesting that these supernatants are enriched in PSI. It is likely that proteins mainly localized in the stromal lamellae were subjected to the action of the detergent while grana were spun down in the pellet. This is consistent with the lateral heterogeneity model for the distribution of pigment-protein complexes of the thylakoid membranes proposed to isolate intact grana (Anderson and Andersson, 1980 and Morosinotto et al. 2010). At 20 mM with both DM isomers we have obtained 80% of thylakoid solubilization. The supernatant contained: a lower amount of small membrane fragments (more protein complexes entering the native gels), and also medium sized complexes fully solubilized as PSII dimers and PSI–LHCI sup ercomplexes they have been identified in the BN-PAGE. At this concentration we suggest that complexes localized in the stroma lamellae and also grana margins/margin ends were subjected to the detergent action, in accordance with findings obtained by van Roon and his co-workers (van Roon et al. 2000).

With a concentration of 30 mM or above with both DM isomers, brought about the total solubilization of thylakoids (also PSII dimers, PSI–LHCI and PSII–LHCII supercomplexes were isolated). We suggest that both detergents, at this concentration, have access the grana regions and solubilize large pigment-protein complexes. This conclusion is consistent with previous results where β-DM was used

at a Chl/DM ratio of 1:40 to isolate PSII–LHCII supercomplexes directly from spinach thylakoids (Eshaghi et al. 1999). In summary, our study has revealed that, it is possible to isolate in different amounts fully solubilized ATP-ase, Cyt b6/f, PSI and PSII complexes either in protomeric or different self-associated states depending on the type of detergent used (α-DM or β-DM) and its concentration (between 5 and 100 mM). This experimental evidence corroborates the idea that different interaction/penetration into the membranes of the two DM isomers, due to the their different chemical properties of both isomers, have a drastical effects on the thylakoids solubilization. We have demonstrated infact, that the two isomeric forms of DM, when compared at the same thylakoids Chl/DM ratio, α-DM is a milder detergent than β-DM, preserving the integrity even of the largest pigment-protein supercomplexes embedded into the thylakoids membranes. Moreover we have identified in 50 mM the minimal concentration that fully solubilize PSII-LHCII supercomplexes.

4.2 Characterization of PSII-LHCII supercomplexes isolated from pea thylakoid membranes by one-step treatment with α- and β-dodecyl-D-maltoside.

In this second work we have optimized the conditions to obtain homogeneous preparations, by using as detergents the two DM isomers α and β, of the C_2S_2 and $C_2S_2M_2$ PSII-LHCII supercomplexes and biochemically and structurally characterized them in agreement with the preavious results obtained by Boekema and his co-workers (Boekema et al. 1999a).

We have found that unlike C_2S_2, the $C_2S_2M_2$ supercomplex contained both the Lhcb3 and Lhcb6 antennae subunits, crucial polypeptides for the assembly and the macro organization of this supercomplex in the thylakoid membrane of higher plants (Caffarri et al. 2009). Both supercomplexes isolated contain the intrinsic protein PsbW and the extrinsic protein PsbO but only the $C_2S_2M_2$ contains also detectable levels of PsbP, PsbQ and PsbR. Our analyses of a and b particles by negative stain EM and interpretation of density within the top-view projections using currently available X-ray data confirmed the protein compositions suggested previously of both supercomplexes (Dekker and Boekema, 2005). We have identified infact density for two types of LHCII trimers designated as S and M, where S, common to both supercomplexes, consists of Lhcb1 and Lhcb2 proteins, whereas M, exclusive to the α particle, is a LHCII trimer containing the Lhcb3 protein. These results are in

accordance with previous findings suggesting that Lhcb3 is a subunit of the M-trimer (Boekema et al. 1999b)

We have carried out the same fitting of the crystal structures into the electron density as proposed in Caffarri et al. 2009 except for small rotational adjustments of CP24 and CP26, although the reliability of the fitting must be treated with caution. In modelling the organization of the subunits within the supercomplex, we used the latest X-ray data for the PSII dimeric core (Umena et al. 2011), LHCII trimer (Standfuss et al. 2005) and CP29 (Pan et al. 2011).We conclude, that Lhcb4 is likely to be located close to the M-trimer in $C_2S_2M_2$ and linked to it via Lhcb6.

4.3 Proteomic characterization and three dimensional electron microscopy study of PSII-LHCII supercomplexes from higher plants.

In this third work we have conducted an in-depth polypeptide composition characterization of PSII-LHCII supercomplexes $C_2S_2M_2$ and C_2S_2 preaviously characterized. Moreover we have obtained the first 3D map of $C_2S_2M_2$.

The biochemical results shown that both supercomplexes have an identical set of LMM subunits. Thus, we conclude that among the identified LMM subunits none is specifically required for the binding of the additional LHCII M-trimers to the basic C_2S_2 unit. In contrast to the LMM subunits, the two isolated supercomplexes revealed basic differences in their Lhcb antennae polypeptides: Lhcb1, Lhcb2, Lhcb4 and Lhcb5 were found in both the $C_2S_2M_2$ and C_2S_2 supercomplexes, whereas Lhcb3 and Lhcb6 were present only in the largest supercomplex, suggesting that Lhcb3 is exclusively located in the LHCII M-trimer and Lhcb6 functions as a linker for this LHCII trimer to the C_2S_2.

The proteomic data indicate that, in addition to the PsbO subunit, which is stably bound to the PSII RC core in both types of supercomplexes, the $C_2S_2M_2$ supercomplex retains partially the PsbP, PsbQ and PsbR subunits.

The EM analysis have allowed to obtained the first 3D structural model of an isolated $C_2S_2M_2$ supercomplex with a resolution of approximately 30 Å according to the 3sFSC criterion. Our model confirms the central positioning of the C_2S_2 supercomplex within the volume of the $C_2S_2M_2$ molecular envelope and the relative positioning of various major subunits. The modeling in our corresponding 3D

electron density map is very similar to that proposed by Caffarri et al. 2009. Unfortunately the dataset which we have used was poor of tilted view particles and it hasn't allowed to resolve the density for the OEC proteins. So it is difficult to suggest the location of the PsbP, PsbQ and PsbR subunits. An improved dataset, ideally derived from cryo-TEM, will be required to resolve and assign the OEC proteins to gain fine details of the overall structure of the $C_2S_2M_2$ supercomplex.

REFERENCES

Anbudurai, P.R. and Pakrasi, H.B. (1993). Mutational analysis of the PsbL protein of photosystem II in the cyanobacterium Synechocystis sp. PCC 6803. *Z. Naturforsch C.* 48:267-274.

Anderson, J. M. (1975). The molecular organization of chloroplast thylakoids. *Biochim. Biophys. Acta* 416:191-235.

Andersson, B. and Anderson, J. M. (1980). Lateral heterogeneity in the distribution of chlorophyll-protein complexes of the thylakoid membranes of spinach chloroplasts. *Biochim. Biophys. Acta* 593:427-440.

Arnon, D.J. (1949). Copper enzymes in isolated chloroplast polyphenoloxydase in Beta vulgaris. *Plant Physiol.* 24:1-14.

Arnon, D.I., Allen, M.B., Whatley, F.R. (1954). Photosynthesis by isolated chloroplasts. *Nature* 174:394-396.

Aspinall-O'Dea, M., Wentworth, M., Pascal, A., Robert, B., Ruban, A., Horton, P. (2002). In vitro reconstitution of the activated zeaxanthin state associated with energy dissipation in plants. *Proc. Natl. Acad. Sci. USA* 99:16331-16335.

Austin, J.R., Staehelin, L.A. (2011). Three-dimensional architecture of grana and stroma thylakoids of higher plants as determined by electron tomography. *Plant Physiol.* 155:1601-1611.

Balsera, M., Arellano, J.B., Revuelta, J.L., de las Rivas, J., Hermoso, J.A. (2005). The 1.49 Å resolution crystal structure of PsbQ from photosystem II of Spinacia oleracea reveals a PPII structure in the N-terminal region. *J. Mol. Biol.* 350:1051-1060.

Barbato, R., Friso, G., Rigoni, F., Dalla Vecchia, F., Giacometti, G.M. (1992). Structural changes and lateral redistribution of Photosystem II during donor side photoinhibition of thylakoids. *J. Cell Biol.* 119:325-335.

Barber, J. (1987). Photosynthetic reaction centres - a common link. *Trends Biochem. Sci.* 12:32-326.

Barber, J. (2006). Photosystem II: An enzyme of global significance. *Biochem. Soc. Trans.* 34:619-631.

Barera, S., Pagliano, C., Pape, T., Saracco, G., Barber, J. (2012). Characterization of PSII-LHCII supercomplexes isolated from pea thylakoid membrane by one-step treatment with α- and β-dodecyl-D-maltoside. *Phil. Trans. R. Soc. B* 367:3389-3399.

Bäverbäck, P., Oliveira, C.L.P., Garamus, V.M., Varga, I., Claesson, P.M., Pedersen, J.S. (2009). Structural properties of β-dodecylmaltoside and C12E6 mixed micelles. *Langmuir* 25:7296-7303.

Bergantino, E., Segalla, A., Brunetta, A., Teardo, E., Rigoni, F., Giacometti, G. M., Szabò, I. (2003). Light- and pH-dependent structural changes in the PsbS subunit of photosystem II. *Proc. Natl. Acad. Sci. USA* 100:15265-15270.

Bishop, C.L., Ulas, S., Baena-Gonzalez, E., Aro, E.M., Purton, S., Nugent, J.H., Mäenpää, P. (2007). The PsbZ subunit of photosystem II in Synechocystis sp. PCC 6803 modulates electron flow through the photosynthetic electron transfer chain. Photosynth. Res. 93:139-147.

Boardman, N.K., and Anderson, J.M. (1964). Isolation from spinach chloroplasts of particles containing different proportions of chlorophyll a and chlorophyll b and their possible role in the light reactions of photosynthesis. *Nature* 203:166-167.

Boekema, E.J., van Roon, H., Calkoen, F., Bassi, R., Dekker, J.P. (1999a). Multiple types of association of photosystem II and its light-harvesting antenna in partially solubilized photosystem II membranes. *Biochemistry* 38:2233-2239.

Boekema, E.J., van Roon, H., van Breemen, J.F.L., Dekker, J.P. (1999b). Supramolecular organization of photosystem II and its light-harvesting antenna in partially solubilized photosystem II membranes. *Eur. J. Biochem.* 266:444–452.

Boekema, E.J., van Breemen, J.F.L., van Roon, H., Dekker, J.P. (2000). Conformational changes in photosystem II supercomplexes upon removal of extrinsic subunits. *Biochemistry* 39:12907-12915.

Bricker, T.M. (1992). Oxygen evolution in the absence of the 33-kilodalton manganese-stabilizing protein. *Biochemistry* 31:4623-4628.

Bricker, T.M., Roose J.L., Fagerlund, R.D., Frankel, L.K., Eaton-Rye, J.J. (2012). The extrinsic proteins of photosystem II. *Biochim. Biophys. Acta* 1817:121-142.

Büchel, C., Morris, E., Orlova, E., Barber. J. (2001). Localisation of the PsbH subunit in photosystem II: a new approach using labelling of Histags with a Ni^{2+}-NTA gold cluster and single particle analysis. *J. Mol. Biol.* 312:371-379.

Bumba, L., Husak, M., Vacha, F. (2004). Interaction of photosystem 2-LHC2 supercomplexes in adjacent layers of stacked chloroplast thylakoid membranes. *Photosynthetica* 42:19-199.

Caffarri, S., Kouril, R., Kereïche, S., Boekema, E.J., Croce , R. (2009). Functional architecture of higher plant photosystem II supercomplexes. *EMBO J.* 28: 3052-3063.

Calderone, V., Trabucco, M., Vujicic, A., Battistutta, R., Giacometti, G.M., Andreucci, F., Barbato, R., Zanotti, G. (2003). Crystal structure of the PsbQ protein of photosystem II from higher plants. *EMBO Rep.* 4:900-906.

Cecutti, C., Focher, B., Perly, B., Zemb, T. (1991). Glycolipid self-assembly: micellar structure. *Langmuir* 7:2580-2585.

DalCorso, G., Pesaresi, P., Masiero, S., Aseeva, E._, Schunemann, D., Finazzi, G., Joliot, P., Barbato, R., Leister, D. (2008). A complex containing PGRL1 and PGR5 is involved in the switch between linear and cyclic electron flow in Arabidopsis. *Cell* 132:273-285.

Danielsson, R., Suorsa, M., Paakkarinen, V., Albertsson, P.E., Styring, S., Aro, E.M., Mamedov, F. (2006). Dimeric and monomeric organization of photosystem II. *J. Biol. Chem.* 281:14241-14249.

Daum, B., Nicastro, D., Austin, J., McIntosh, J., Kühlbrandt, W. (2010). Arrangement of photosystem II and ATP synthase in chloroplast membranes of spinach and pea. *Plant Cell* 22:1299-1312.

Deisenhofer, J., Epp, O., Miki, R.H., Huber, R., Michel, H. (1985). Structure of the protein subunits in the photosynthetic reaction centre of Rhodopseudomonas viridis at 3-2 resolution. *Nature* 318:618-624.

Dekker, J.P., and Boekema, E.J. (2005). Supramolecular organization of thylakoid membrane proteins in green plants. *Biochim. Biophys. Acta* 1706:12-39.

De Grip, W.J. (1982). Thermal stability of rhodopsin and opsin in some novel detergents. *Methods Enzymol*. 81:256-265.

De Las Rivas, J., and Barber, J. (2004). Analysis of the structure of the PsbO protein and its implications. *Photosynth. Res.* 81:329-343.

De Las Rivas, J., and Roman, A. (2005). Structure and evolution of the exstrinsic proteins that stabilize the oxygen-evolving engine. *Photochem. Photobiol. Sci.* 4:1003-1010.

Dominici, P., Caffarri, S., Armenante, F., Ceoldo, S., Crimi, M., Bassi, R. (2002). Biochemical properties of the PsbS subunit of photosystem II either purified from chloroplast or recombinant. *J. Biol. Chem.* 277:22750-22758.

Enami, I., Suzuki, T., Tada, O., Nakada, Y., Nakamura, K., Tohri, A., Ohta, H., Inoue, I., Shen, J.R. (2005). Distribution of the extrinsic proteins as a potential marker for the evolution of photosynthetic oxygen-evolving photosystem II. *FEBS J.* 272:5020-5030.

Enami, I., Okumura, A., Nagao, R., Suzuki, T., Iwai, M., Shen J. (2008). Structures and functions of the extrinsic proteins of photosystem II from different species. *Photosynth. Res.* 98:349-63.

Eshaghi, S., Andersson, B. & Barber, J. (1999). Isolation of a highly active PSII–LHCII supercomplex from thylakoid membranes by a direct method. *FEBS Lett.* 446:23-26.

Ferreira, K.N., Iverson, T.M., Maghlaoui, K., Barber, J., Iwata, S. (2004). Architecture of the photosyntetic oxygen-evolving center. *Science* 303:1831-1838.

Funk, C.C. (2000). Functional analysis of the PsbX protein by deletion of the corresponding gene in Synechocystis sp. PCC 6803. *Plant Mol. Biol*. 44:815-827.

Funk C.C., Schröder, W.P., Napiwotzki, A., Tjus, S.E., Renger, G., Andersson, B. (1995). The PSII-S protein of higher plants: a new type of pigment-binding protein. *Biochemistry* 34:11133-11141.

García-Cerdán, J.G., Kovács, L., Tóth, T., Kereïche, S., Aseeva, E., Boekema, E.J., Mamedov, F., Funk, C., Schröder, W.P. (2011). The PsbW protein stabilizes the supramolecular organization of photosystem II in higher plants. *Plant J*. 65:368-38.

Gau, A.E., Thole, H.H., Sokolenko, A., Altschmied, L., Herrmann, R.G., Pistorius, E.K. (1998). PsbY, a novel manganese-binding, lowmolecular-mass protein associated with photosystem II. *Mol. Gen. Genet.* 260:56-68.

Ghanotakis, D.F., Topper J.N., Yocum, C.F. (1984). Structural organization of the oxidizing side of photosystem II. Exogenous reductants reduce and destroy the Mn-complex in photosystems II membranes depleted of the 17 and 23 kDa polypeptides. *Biochim. Biophys. Acta* 767:524-531.

Guskov, A., Kern, J., Gabdulkhakov, A., Broser, M., Zouni, A., Saenger, W. (2009). Cyanobacterial photosystem II at 2.9 Å resolution and the role of quinones, lipids, channels and chloride. *Nat. Struct. Mol. Biol.* 16:334-342.

Hankamer, B., Nield, J., Zheleva, D., Boekema, E., Jansson, S., Barber, J. (1997). Isolation and biochemical characterisation of monomeric and dimeric photosystem I1 complexes from spinach and their relevance to the organisation of photosystem II in vivo. *Eur. J. Biochem.* 243:422-429.

Heber, U., Kirk, M.R., Boardman, N.K. (1979). Photoreactions of Cytochrome b-559 and cyclic electron flow in photosystem II of intact chloroplasts. *Biochim. Biophys. Acta* 546:292-306.

Hellmann, U., Wernstedt, C., Gonez, J., Heldin, C.H. (1995). Improvement of an "In-Gel" digestion procedure for the micropreparation of internal protein fragments for amino acid sequencing. *Anal. Biochem.* 224:451-455.

Ido, K., Ifuku, K., Yamamoto, Y., Ishihara, S., Murakami, A., Takabe, K., Miyake, C., Sato, F. (2009). Knockdown of the PsbP protein does not prevent assembly of the dimeric PSII core complex but impairs accumulation of photosystem II supercomplexes in tobacco. *Biochim. Biophys. Acta* 1787:873-881.

Ifuku, K. and Sato, F. (2001). Importance of the N-terminal sequence of the extrinsic 23 kDa polypeptide in photosystem II in ion-retention in oxygen-evolution. *Biochim. Biophys. Acta* 1546:196-204.

Ifuku, K., Nakatsu, T., Kato, H., Sato, F. (2004). Crystal structure of the PsbP protein of photosystem II from *Nicotiana tabacum*. *EMBO rep.* 5:362-368.

Ikeuchi, M., Koike, H., Inoue, Y. (1989). N-terminal sequencing of lowmolecular-mass components in cyanobacterial photosystem II core complex. Two components correspond to unidentified open reading frames of plant chloroplast DNA. *FEBS Lett.* 253:178-182.

Ikeuchi, M., Shukla, V.K., Pakrasi, H.B., Inoue, Y. (1995). Directed inactivation of the psbI gene does not affect photosystem II in the cyanobacterium Synechocystis sp. PCC 6803. *Mol. Gen. Genet.* 249:622-8.

Ishihara, S., Yamamoto, Y., Ifuku, K., Sato, F. (2005). Functional analysis of four members of the PsbP family in Photosystem II in Nicotiana tabacum using differential RNA interference. *Plant Cell Physiol*. 46:1885-1893.

Ishihara, S., Takabayashi, A., Ido, K., Endo, T., Ifuku, K., Sato, F. (2007). Distinct functions for the two PsbP-like proteins PPL1 and PPL2 in the chloroplast thylakoid lumen of Arabidopsis. *Plant Physiol*. 145:668-679.

Jansson, S. (1999). A guide to the Lhc genes and their relatives in Arabidopsis. *Trends Plant Sci*. 4: 236-240.

Jackowski, G., Olkiewicz, P., and Zelisko, A. (2003). The acclimative response of the main light-harvesting chlorophyll a/b-protein complex of photosystem II (LHCII) to elevated irradiances at the level of trimeric subunits. *J. Photochem. Photobiol.* 70:163-70.

Jones, M.N. (1999). Surfactants in membrane solubilisation International Journal of Pharmaceutics 177:137-159.

Jordan, P., Fromme, P., Witt, H.T., Klukas, O., Saenger, W., Krauß, N. (2001). Three-dimensional structure of cyanobacterial photosystem I at 2.5 Å resolution. *Nature* 411:909-917.

Kamiya, N. and Shen, J.R. (2003). Crystal structure of oxygen-evolving photosystem II from *Thermosynechococcus vulcanus* at 3.7 Å resolution. *Proc. Natl. Acad. Sci. USA* 100:98-103.

Kashino,Y., Koike, H., Satoh, K. (2001). An improved sodium dodecyl sulfate-polyacrylamide gel electrophoresis system for the analysis of membrane protein complexes. *Electrophoresis* 22:1004-1007.

Kashino, Y., Koike, H., Yoshio, M., Egashira, H., Ikeuchi, M., Pakrasi, H.B., Satoh, K. (2002). Low molecular-mass polypeptide components of a photosystem II preparation from the thermophilic cyanobacterium *Thermosynechococcus vulcanus*. *Plant Cell Physiol.* 43:1366-1373.

Kim, S.J. Robinson, D., Robinson, C. (1996). An Arabidopsis thaliana cDNA encoding PS II-X, a 4.1 kDa component of photosystem II: a bipartite presequence mediates SecA/delta pH-independent targeting into thylakoids. *FEBS Lett.* 390:175-178.

Kirchhoff, H., Haase, W., Wegner, S., Danielsson, R., Ackermann, R., Albertsson, P.A. (2007). Low-light-induced formation of semicrystalline photosystem II arrays in higher plant chloroplasts. *Biochemistry* 46:11169-11176.

Kiss, A.Z., Ruban, A.V., Horton, P. (2008). The PsbS protein controls the organization of the photosystem II antenna in higher plant thylakoid membranes. *J. Biol. Chem.* 283:3972-3978

Kovacs, L., Damkjær, J., Kereïche, S., Ilioaia, C., Ruban, A., Boekema, E.J., Jansson, S., Horton, P. (2006). Lack of the light-harvesting complex CP24 affects the structure and function of the grana membranes of higher plant chloroplasts. *Plant Cell* 18:3106-3120.

Kruse, O., Zheleva, D., Barber, J. (1997). Stabilization of photosystem two dimers by phosphorylation: implication for the regulation of the turnover of D1 protein. *FEBS Lett.* 408:276-280.

Laemmli, U.K. (1970). Cleavage of structural proteins during the assembly of the head of bacteriophage T4. *Nature* 227:680-685.

Lautner, A., Klein, R., Ljungberg, U., Reiländer, H., Bartling, D., Andersson, B., Reinke, H., Beyreuther, K., Herrmann, R.G. (1988). Nucleotide sequence of cDNA clones encoding the complete precursor for the ‘‘10-kDa’’ polypeptide of photosystem II from spinach. *J. Biol. Chem.* 263:10077-10081.

Li, X.P., Björkman, O., Shih, C., Grossman, A.R., Rosenquist, M., Jansson, S., Niyogi, **K.K.** (2000). A pigment-binding protein essential for regulation of photosynthetic light harvesting. *Nature* 403:391-395.

Lind, L.K., Shukla, V.K., Nyhus, K.J., Pakrasi, H.B. (1993). Genetic and immunological analyses of the cyanobacterium Synechocystis sp. PCC 6803 show that the protein encoded by the psbJ gene regulates the number of photosystem II centers in thylakoid membranes. *J. Biol. Chem.* 268:1575-1579.

Liu, Z.F., Yan, H.C., Wang, K.B., Kuang, T.Y., Zhang, J.P., Gui, L.L., An, X.M., Chang, W.R. (2004). Crystal structure of spinach major light-harvesting complex at 2.72 Å resolution. *Nature* 428: 287-292.

Loll, B., Kern, J., Saenger, W., Zouni, A., Biesiadka, J. (2005). Towards complete cofactor arrangement in then 3.0 Å resolution structure of photosystem II. *Nature* 438:1040-1044.

Lund, S., Orlowski, S., de Foresta, B., Champeil, P., le Maire, M., Moller, J.V. (1989). Detergent structure and associated lipid as determinants in the stabilization of solubilized Ca^{2+}-ATPase from sarcoplasmic reticulum. *J. Biol. Chem.* 264:4907-4915.

Lundin, B., Thuswaldner, S., Shutova, T., Eshaghi, S., Samuelsson, G., Barber, J., Andersson, B., Spetea, C. (2007). Subsequent events to GTP binding by the plant PsbO protein: structural changes, GTP hydrolysis and dissociation from the photosystem II complex. *Biochim. Biophys. Acta* 1767:500-508.

Lundin, B., Nurmi, M., Rojas-Stuetz, M., Aro, E.M., Adamska, I., Spetea, C. (2008). Towards understanding the functional difference between the two PsbO isoforms in *Arabidopsis thaliana*-insights of psbo knockout mutants. *Photosynth. Res.* 98:405-414.

Ljungberg, U., Akerlund, H.E., Andersson, B. (1986). Isolation andcharacterization of the 10-kDa and 22-kDa polypeptides of higher plant photosystem 2. *Eur. J. Biochem.* 158:477-482.

Mayes, S.R., Cook, K.M., Self, S.J., Zhang, Z., Barber, J. (1991). Deletion of the gene encoding the Photosystem II 33 kDa protein from Synechocystis sp. PCC 6803 does not inactivate water-splitting but increases vulnerability to photoinhibition. *Biochim. Biophys. Acta.* 1060:1-12.

Mayfield, S., Bennoum, P., Rochaix, J.D. (1987). Expression of the nuclear encoded OEE1 proteins is required for oxygen evolution and stability of photosystem II particles in *Chlamydomonas reinhardtii*. *EMBO J.* 6:313-318.

Meetam, M., Keren, N., Ohad, I., Pakrasi, H.B. (1999). The PsbY protein is not essential for oxygenic photosynthesis in the cyanobacterium Synechocystis sp. PCC 68031. *Plant Physiol.* 121:1267-1272.

Michel, H.P. and Bennett, J. (1987). Identification of the phosphorylation site of an 8.3 kDa protein from photosystem II of spinach. *FEBS Lett.* 212:103-108.

Michel, H.P., Hunt, D.F., Shabanowitz, J., Bennett, J. (1988). Tandem mass spectrometry reveals that three photosystem II proteins of spinach chloroplasts contain N-acetyl-O-phosphothreonine at their NH_2 termini. *J. Biol. Chem.* 263:1123-1130.

Miyao, M., and Murata, N. (1984). Calcium ion can be substituded for the 23-kDa polypeptide in photosynthetic oxygen evolution. *FEBS Lett.* 168:118-120.

Miyao, M. and Murata, N. (1985). The Cl- effect on photosynthetic oxygen evolution: interaction of Cl with 18-kDa, 24-kDa and 33-kDa proteins. *FEBS Lett*. 180:303-308.

Monod, C., Takahashi, Y., Goldschmidt-Clermont, M., Rochaix, J.D. (1994). The chloroplast ycf8 open reading frame encodes a photosystem II polypeptide which maintains photosynthetic activity under adverse growth conditions. *EMBO J.* 13:2747-2754.

Morais, F., Barber, J., Nixon, P.J. (1998). The chloroplast encoded alpha subunit of cytochrome b559 is required for assembly of the PSII complex in both the light and dark in *Chlamydomonas reinhardtii*. *J. Biol. Chem.* 273:29315-29320.

Morosinotto, T., Segalla, A., Giacometti, G.M., Bassi, R. (2010). Purification of structurally intact grana from plants thylakoids membranes. *J. Bioenerg. Biomembr.* 42:37-45.

Mulo, P., Sirpio, S., Suorsa, M., Aro, E. M. (2008). Auxiliary proteins involved in the assembly and sustenance of photosystem II. *Photosynth. Res.* 98:489-501.

Murakami, R., Ifuku, K., Takabayashi, A., Shikanai, T., Endo, T., Sato, F. (2002). Characterization of an *Arabidopsis thaliana* mutant with impaired psbO, one of genes encoding 33-kDa protein of oxygen-evolving complex, which shows retarded growth. *FEBS Lett.* 523:138-142.

Murakami, R., Ifuku, K., Takabayashi, A., Shikanai, T., Endo, T., Sato, F. (2005). Functional dissection of two Arabidopsis PsbO proteins PsbO1 and PsbO2. *FEBS J.* 272:2165-2175.

Murray, J.W., Maghlaoui, K., Kargul, J., Ishida, N., Lai, T.L., Rutherford, A.W., Sugiura, M., Boussac, A., Barber, J. (2008). X-ray crystallography identifies two chloride binding sites in the oxygen evolving centre of photosystem II. *Energy Environ. Sci.* 1:161–166.

Mustàrdy, L., Buttle, K., Steinbach, G., Garab, G. (2008). The three-dimensional network of the thylakoid membranes in plants: Quasihelical model of the granum-stroma assembly. *Plant Cell* 20:2552-2557.

Nanba, O. and Satoh, K. (1987). Isolation of a photosystem II reaction center consisting of D1 and D2 polypeptides and cytochrome b559. *Proc. Natl. Acad. Sci. USA* 84:109-112.

Nield, J., Balsera, M., De Las Rivas, J., Barber, J. (2002). Three-dimensional electron cryo-microscopy study of the extrinsic domains of the oxygen-evolving complex of spinach. Assignment of the PsbO protein. *J. Biol. Chem.* 277:15006-15012.

Nield, J. and Barber, **J.** (2006). Refinement of the structural model for the photosystem II supercomplex of higher plants. *Biochim. Biophys. Acta* 1757:353-361.

Ohnishi, N. and Takahashi, Y. (2001). PsbT polypeptide is required for efficient repair of photodamaged photosystem II reaction center. *J. Biol. Chem.* 276:33798-33804.

Pagliano, C., Raviolo, M., Dalla Vecchia, F., Gabbrielli, R., Gonnelli, C., Rascio, N., Barbato, R., La Rocca, N. (2006). Evidence for PSII donor-side damage and photoinhibition induced by cadmium treatment on rice (Oryza sativa L.). *J. Photochem. Photobiol.* 84:70-78.

Pagliano, C., La Rocca, N., Andreucci, F., Deak, S., Vass, I., Rascio, N., Barbato, R. (2009). The extreme halophyte *Salicornia veneta* is depleted of the extrinsic PsbQ and PsbP proteins of the oxygen-evolving complex without loss of functional activity. *Ann. Bot.* 103:505-515.

Pagliano, C., Chimirri, F., Saracco, G., Marsano, F., Barber, J. (2011). One-step isolation and biochemical characterization of a highly active plant PSII monomeric core. *Photosynth. Res.* 108:33-46.

Pan, X., Li, M., Wan, T., Wang, L., Jia, C., Hou, Z., Zhao, X., Zhang, J., Chang, W. (2011). Structural insights into energy regulation of light-harvesting complex CP29 from spinach. *Nat. Struct. Mol. Biol.* 18:309-316.

Peltier, J.B., Friso, G., Kalume, D.E., Roepstorff, P., Nilsson, F., Adamska, I., van Wijk, K.J. (2000). Proteomics of the chloroplast: systematic identification and targeting analysis of lumenal and peripheral thylakoid proteins. *Plant Cell* 12:319-341.

Peltier, G., and Cournac, L. (2002). Chlororespiration. *Annu. Rev. Plant Biol.* 53:523-550.

Pettersen, E.F., Goddard, T.D., Huang, C.C., Couch, G.S., Greenblatt, D.M, Meng, E.C., Ferrin, T.E. (2004). UCSF Chimera–A visualization system for exploratory research and analysis. *J. Comput. Chem.* 25:1605-1612.

Philbrick, J.B., Diner, B.A., Zilinskas, B.A. (1991). Construction and characterization of cyanobacterial mutants lacking the manganese-stabilizing polypeptide of photosystem II. *J. Biol. Chem.* 266:13370-13376.

Popelkova, H., Im, M.M., D'Auria, J., Betts, S.D., Lydakis-Simantiris, N., Yocum, C.F. (2002 a). N-terminus of the photosystem II manganese stabilizing protein: effects of sequence elongation and truncation. *Biochemistry* 41:2702-11.

Popelkova, H., Im, M.M., Yocum, C.F. (2002 b). N-terminal truncations of manganese stabilizing protein identify two amino acid sequences required for binding of the eukaryotic protein to photosystem II and reveal the absence of one binding- related sequence in cyanobacteria. *Biochemistry* 41:10038-10045.

Poulson, M. Samson, G. Whitmarsh, J. (1995). Evidence that cytochrome b 559 protects photosystem II against photoinhibition, Biochemistry 34:10932-10938.

Pursiheimo, S., Rintamäki, E., Baena-Gonzales, E., Aro, E.M. (1998). Thylakoid protein phosphorylation in evolutionally divergent species with oxygenic photosynthesis. *FEBS Lett*. 423:178-182.

Radermacher, M. (1988). Three-dimensional reconstruction of single particles from random and nonrandom tilt series. *J. Electron. Microsc. Tech.* 9:359-394.

Regel, R.E., Ivleva, N.B., Zer, H., Meurer, J., Shestakov, S.V., Herrmann, R.G., Pakrasi, H.B., Ohad, I. (2001). Deregulation of electron flow within photosystem II in the absence of the PsbJ protein. *J. Biol. Chem.* 276:41473-41478.

Roose, J.L., Wegener, K.M., Pakrasi, H.B. (2007a). The extrinsic proteins of photosystem II. *Photosynth. Res.* 92:369-387.

Roose, J.L., Kashino, Y., Pakrasi, H.B. (2007b). The PsbQ protein defines cyanobacterial photosystem II complexes with highest activityand stability. *Proc. Natl. Acad. Sci. USA* 104:2548-2553.

Rossmann, M.G. (2000). Fitting atomic models into electron-microscopy maps. *Acta Crystallogr.* 56:1341-1349.

Ruban, A.V., Wentworth, M., Yakushevska, A.E., Andersson, J., Lee, P.J., Keegstra, W., Dekker, J.P., Boekema, E.J., Jansson, S., Horton., P. (2003). Plants lacking the main lightharvesting complex retain photosystem II macro-organization. *Nature* 421:648-652.

Sardet, C. Tardieu, A. Luzzati,V. (1976). Shape and size of bovine rhodopsin-small angle X-ray scattering study of a rhodopsin detergent complex. *J. Mol. Biol.* 105:383-407.

Schägger, H., and von Jagow, G. (1987). Tricine-sodiumdodecyl sulfate-polyacrylamide gel electrophoresis for the separation of proteins in the range from 1 to 100 kDa. *Anal. Biochem.* 166:368-379.

Schubert, M., Petersson, U.A. Haas, B.J., Funk, C., Schroder, W.P., Kieselbach, T. (2002). Proteome map of the chloroplast lumen of Arabidopsis thaliana. *J. Biol. Chem.* 277:8354-8365.

Seidler, A. (1996). The extrinsic polypeptides of Photosystem II. *Biochim. Biophys. Acta* 1277:35-60.

Shi, L.X., Kim, S.J., Marchant, A., Robinson, C., Schröder, W.P. (1999). Characterisation of the PsbX protein from photosystem II and light regulation of its gene expression in higher plants. *Plant Mol. Biol.* 40:737-744.

Shi, L.X., Schröder, W.P. (2004) The low molecular mass subunits of the photosynthetic supracomplex, photosystem II. *Biochim. Biophys. Acta* 1608:75-96

Shikanai, T. (2007). Cyclic electron transport around Photosystem I: genetic approaches. *Annu Rev Plant Biol.* 58: 199-217.

Shimoni, E., Rav-Hon, O., Ohad, I., Brumfeld, V., Reich, Z. (2005). Three-dimensional organization of higher-plant chloroplast thylakoid membranes revealed by electron tomography. *Plant Cell* 17:2580-2586.

Staehelin, L.A. and van der Staay, G.W.M. (1996). Structure, composition, functional organisation and dynamic properties of thylakoid membranes, in Oxygenic Photosynthesis: The Light Reactions (eds. Ort, D.R., Yocum, C.F.), pp. 11–30, Dordrecht, NT: Kluwer Academic Publishers.

Staehelin, A.(2003). Chloroplast structure: from chlorophyll granules to supra-molecular architecture of thylakoid membranes. *Photosynth. Res.* 76:185-196.

Standfuss, J., van Scheltinga, A.C.T., Lamborghini, M., Kühlbrandt, **W.** (2005). Mechanisms of photoprotection and nonphotochemical quenching in pea light harvesting complex at 2.5 Å resolution. *EMBO J.* 24:918-928.

Sugimoto, I. and Takahashi, Y. (2003). Evidence that the PsbK polypeptide is associated with the photosystem II core antenna complex CP43. *J. Biol. Chem.* 278:45004-45010.

Suzuki, T., Minagawa, J., Tomo, T., Sonoike, K., Ohta, H., Enami, I. (2003). Binding and functional properties of the extrinsic proteins in oxygen-evolving photosystem II particle from a green alga, *Chlamydomonas reinhardtii* having His-tagged CP47. *Plant Cell Physiol*. 44:76-84.

Swiatek, M., Kuras, R., Sokolenko, A., Higgs, D., Olive, J., Cinque, G., Müller, B., Eichacker, L.A., Stern, D.B., Bassi, R., Herrmann, R.G., Wollman, F.A. (2001). The chloroplast gene ycf9 encodes a photosystem II (PSII) core subunit, PsbZ, that participates in PSII supramolecular architecture. *Plant Cell* 13:1347-1367.

Takahashi, Y., Matsumoto, H., Goldschmidt-Clermont, M., Rochaix, J.D. (1994). Directed disruption of the Chlamydomonas chloroplast psbK gene destabilizes the photosystem II reaction center complex. *Plant Mol. Biol.* 24:779-788.

Takahashi, S., Milward, S.E., Fan, D-Y., Chow, W.S., Badger, M.R. (2009). How does cyclic electron flow alleviate photoinhibition in Arabidopsis? *Plant Physiol.* 149:1560-1567.

Takishita, K., Uchida, A. (1999). Molecular cloning and nucleotide sequence analysis of psbA from dinoflagellates: origin of the dinoflagellate plastid. *Phycol. Res.* 43:207-216.

Tang, G., Peng, L., Baldwin, P.R., Mann, D.S., Jiang, W., Rees, I., Ludtke, S.J. (2007). EMAN2: an extensible image processing suite for electron microscopy.*J. Struct. Biol.* 157:38-46.

Teardo, E., de Laureto, P.P., Bergantino, E., Dalla Vecchia, F., Rigoni, F., Szabò, I., Giacometti, G.M. (2007). Evidences for interaction of PsbS with photosynthetic complexes in maize thylakoids. *Biochim. Biophys. Acta* 1767:703-711.

Tomo, T., Enami, I., Satoh, K. (1993). Orientation and nearest neighbor analysis of psbI gene product in the photosystem II reaction center complex using bifunctional cross-linkers. *FEBS Lett.* 323:15-18.

Thornton, L.E., Ohkawa, H., Roose, J.L., Kashino, Y., Keren, N., Pakrasi, H.B. (2004). Homologs of plant PsbP and PsbQ proteins are necessary for regulation of photosystem II activity in the cyanobacterium Synechocystis 6803. *Plant Cell* 16:2164-2175.

Trotta, A., Redondo-Gòmez, S., Pagliano, C., Clemente, M. E., Rascio, N., Rocca, N. L., Antonacci, A., Andreucci, F., Barbato, R. (2012). Chloroplast ultrastructure and thylakoid polypeptide composition are affected by different salt concentrations in the halophytic plant *Arthrocnemum macrostachyum*. *J. Plant Physiol.* 169:111-116.

Turkina, M.V., Kargul, J., Blanco-Rivero, A., Villarejo, A., Barber, J., Vener, A.V. (2006). Environmentally modulated phosphoproteome of photosynthetic membranes in the green alga *Chlamydomonas reinhardtii*. *Mol. Cell Proteomics* 5:1412-1425.

Xu, Q., Bricker, T.M. Structural organization of proteins on the oxidizing side of photosystem II. Two molecules of the 33-kDa manganese-stabilizing proteins per reaction center. *J Biol Chem.* 1992 Dec 25;267(36):25816-21.

Yakushevska, A.E., Jensen, P.E., Keegstra, W., van Roon, H., Scheller, H.V., Boekema, E.J., Dekker, J.P. (2001). Supermolecular organization of photosystem II and its associated light-harvesting antenna in *Arabidopsis thaliana. Eur. J. Biochem.* 268:6020-6028.

Yan, H., Zhang, P., Wang, C., Liu, Z., Chang, W. (2007). Two lutein molecules in LHCII have different conformations and functions: Insights into molecular mechanism of thermal dissipation plants. *Biochem. Biophys. Res. Commun.* 355:457-463.

Yi, X., McChargue, M., Laborde, S., Frankel, L.K., Bricker, T.M. (2005). The manganese-stabilizing protein is required for photosystem II assembly/stability and photoautotrophy in higher plants. *J. Biol. Chem.* 280:16170-16174.

Yi, X., Hargett, S.R., Frankel, L.K., Bricker, T.M. (2009) The PsbP protein, but not the PsbQ protein, is required for normal thylakoid architecture in Arabidopsis thaliana. *FEBS Lett.* 583:2142-2147.

Umate, P., Schwenkert, S., Karbat, I., Dal Bosco, C., Mlcòchová, L., Volz, S., Zer, H., Herrmann, R.G., Ohad, I., Meurer, J. (2007). Deletion of PsbM in tobacco alters the Q B site properties and the electron flow within photosystem II. *J. Biol. Chem.* 282:9758-9767.

Umena, Y., Kawakami, K., Shen, J.R., Kamiya, N. (2011). Crystal structure of oxygen-evolving photosystem II at a resolution of 1.9 Å. *Nature* 473:55-60.

van Heel, M. (1987). Angular reconstitution: a posteriori assignment of projection directions for 3D reconstruction. *Ultramicroscopy* 21:111-123.

van Heel, M. Schatz, M. (2005). Fourier shell correlation threshold criteria. *J. Struct. Biol.* 151: 250-262.

van Heel, M., Portugal, R., Rohou, A., Linnemayr, C., Bebeacua, C., Schmidt, R., Grant, T., Schatz, M. (2011). Four-dimensional cryo electron microscopy at quasi atomic resolution: 'IMAGIC 4D'. In International tables for crystallography. Vol. F: Crystallography of biological macromolecules (eds M. G. Rossmann, E. Arnold & D. Himmel), pp. 624–628. Chichester, UK: John Wiley and Sons.

van Roon, H., van Breemen, J.F.L., de Weerd, F.L., Dekker, J.P., Boekema, E.J. (2000). Solubilization of green plant thylakoid membranes with n-dodecyl-α-D-maltoside. Implications for the

structural organization of the Photosystem II, Photosystem I, ATP synthase and cytochrome b6/f complexes. *Photosynth. Res*. 64:155–166.

Vener, A.V., Harms, A., Sussman, M.R., Vierstra, R.D. (2001). Mass spectrometric resolution of reversible protein phosphorylation in photosynthetic membranes of *Arabidopsis thaliana*. *J. Biol. Chem.* 276:6959-6966.

Zheleva, D., Sharma, J., Panico, M., Morris, H.R., Barber, J. (1998). Isolation and characterization of monomericand dimeric CP47-reaction center photosystem II complexes. *J. Biol. Chem.* 273:16122-16127.

Zouni, A., Witt, H. T., Kern, J., Fromme, P., Krauss, N., Saenger, W. & Orth, P. (2001). Crystal structure of photosystem II from *Synechococcus elongatus* at 3.8 Å resolution. *Nature* 409:739-743.

PUBLICATIONS IN ATTACHMENT

AKNOWLEDGMENTS

First of all I would like to thank my scientific supervisor Prof. Roberto Barbato for his patience, for teaching me what is science and also my tutor Dott. Cristina Pagliano for all the experiments that she have done, for guiding me during my thesis work, and for teaching me all the biochemical techniques.
I can't forget to thank Prof. James Barber for conveying to me the spark of passion for science.
I wish to thank Dr. Francesco Marsano for his indispensable help in mass spectrometry, Dr. Tillmann Pape and Dr. Jon Nield for the EM analysis.
I would to thank also all my university friends, in particular Alessia my friend and" Ph D mate" for sharing good and bad moments.
I wish to thank my parents for always supported me in my choices.
Last but not least, I would to thank Federica my fiance for supporting me in all situation, for her presence, for her love, that make me more and more "alive" every day.